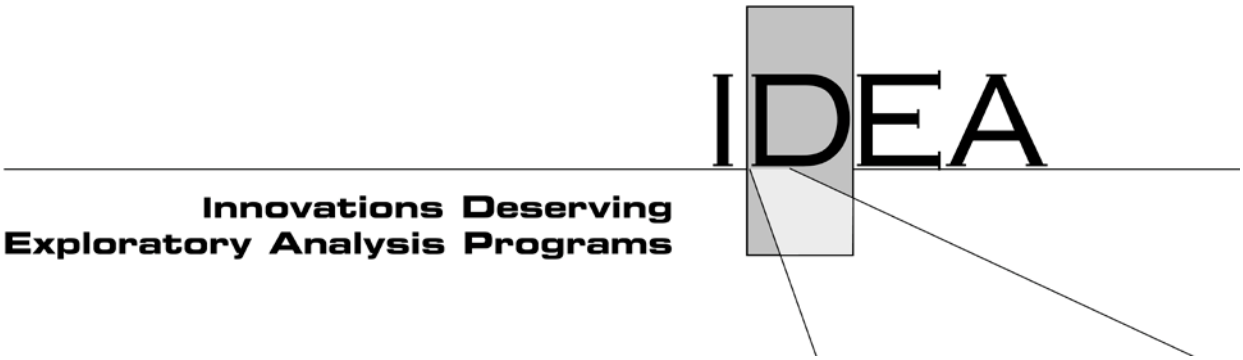

NCHRP IDEA Program

DEVELOPMENT OF THREE POINT BENDING CYLINDER (3PBC) ASPHALT MIXTURE FATIGUE TEST SYSTEM

Final Report for
NCHRP IDEA Project 218

Prepared by:
Aksel Seitllari
Mumtahin Hasnat
M. Emin Kutay
Michigan State University

May 2022

NATIONAL ACADEMIES Sciences Engineering Medicine

TRB TRANSPORTATION RESEARCH BOARD

Innovations Deserving Exploratory Analysis (IDEA) Programs Managed by the Transportation Research Board

This IDEA project was funded by the NCHRP IDEA Program.

The TRB currently manages the following three IDEA programs:

- The NCHRP IDEA Program, which focuses on advances in the design, construction, and maintenance of highway systems, is funded by American Association of State Highway and Transportation Officials (AASHTO) as part of the National Cooperative Highway Research Program (NCHRP).
- The Safety IDEA Program currently focuses on innovative approaches for improving railroad safety or performance. The program is currently funded by the Federal Railroad Administration (FRA). The program was previously jointly funded by the Federal Motor Carrier Safety Administration (FMCSA) and the FRA.
- The Transit IDEA Program, which supports development and testing of innovative concepts and methods for advancing transit practice, is funded by the Federal Transit Administration (FTA) as part of the Transit Cooperative Research Program (TCRP).

Management of the three IDEA programs is coordinated to promote the development and testing of innovative concepts, methods, and technologies.

For information on the IDEA programs, check the IDEA website (www.trb.org/idea). For questions, contact the IDEA programs office by telephone at (202) 334-3310.

IDEA Programs
Transportation Research Board
500 Fifth Street, NW
Washington, DC 20001

DEVELOPMENT OF THREE POINT BENDING CYLINDER (3PBC) ASPHALT MIXTURE FATIGUE TEST SYSTEM

IDEA Program Final Report

Contact Number: NCHRP IDEA 20-30/218

Prepared for the IDEA Program
Transportation Research Board
The National Academies of Sciences,
Engineering and Medicine

by

Aksel Seitllari
Mumtahin Hasnat
M. Emin Kutay (Principal Investigator)

Michigan State University
East Lansing, Michigan

May 18, 2022

ACKNOWLEDGMENTS

The authors are grateful for the assistance provided by the expert panel members: Ali Regimand (InstroTek), Kevin McGhee (Virginia DOT), Matt Corrigan (FHWA), Navneet Garg (FAA) and Walaa Mogawer (Univ. of Massachusetts-Dartmouth) as well as the IDEA program manager Catherine McGhee. In addition, the authors would like to thank Dr. Inam Jawed for his guidance and support during the project. The research team would like to also acknowledge Michigan Asphalt Paving for their benevolent help in providing asphalt mixtures whenever they were needed. Also, many thanks to Brian Gietzel from MSU and Sig Langenberg from the Langenberg Machine Products for their technical supports while building the parts of the fatigue testing fixtures on this project.

Table of Contents

EXECUTIVE SUMMARY

Fatigue cracking is one of the dominant distress types that a pavement structure experiences throughout its service life. The current fatigue cracking tests are lengthy, cumbersome and expensive. Extensive material requirement for sample preparation, difficulty in meeting air void target, a large number of samples needed for testing, common premature 'end-failures' (leading to excessive sample preparation time and consumption of material), and high equipment cost are some of the challenges encountered when running these tests. To overcome some of these shortcomings, researchers from the Advanced Asphalt Characterization Laboratory (AACL) at Michigan State University (MSU) developed a new test method called the 'three-point bending cylinder (3PBC) test'. The primary benefit of this test method is that sample preparation and testing times are shorter than typical fatigue tests (e.g., four-point bending and uniaxial fatigue) and the test fixture is easy to operate and inexpensive. This project was performed in two stages with multiple tasks. Stage 1 of this work focused on the improvement of the design and robustness of the 3PBC fatigue test system, and data analysis methodology. Several enhancements were made to the 3PBC test fixture, which made it easier to work with the Asphalt Mixture Performance Tester (AMPT). In addition, a new testing protocol was programmed in the AMPT to implement the Timoshenko-Ehrenfest Beam Theory formulations. The applicability of Timoshenko-Ehrenfest beam theory formulations to the 3PBC geometry was validated via 3D Viscoelastic Finite Element simulations run at different temperatures and frequencies. In addition, it was shown that the viscoelastic continuum damage (VECD) formulations can be used to analyze the 3PBC data and a single pseudo stiffness (C) versus damage parameter (S) can be obtained from tests at different strain levels, temperatures, and frequencies. This characteristic reduces the experimental burden to compute the number of cycles to failure (Nf) at different strain levels and temperatures. The C versus S curve obtained from a single test, along with the linear viscoelastic dynamic modulus (|E*|) master curve can be used to predict the Nf values at different temperatures, frequencies and strain levels. As a result, phenomenological fatigue life formulation used in Mechanistic-Empirical Pavement Design approaches (e.g., Pavement ME and MEAPA) can be calibrated using a single 3PBC test. In this study, in addition to extensive 3PBC testing, uniaxial fatigue tests were also performed. During the uniaxial fatigue tests, radial strains were measured in addition to the axial strains and the evolution of Poisson's ratio was quantified. In Stage 2, one of the tasks was a ruggedness evaluation of the test setup. The ruggedness testing plan in this study involved: (i) identifying the major test factors that may influence the 3PBC test, and (ii) developing a statistically sound and efficient laboratory experimental design. Two different sets of ruggedness tests were completed. In the first set, geometrical factors (i.e., sample length and diameter) and air void were considered. In the second set, a standardized ruggedness testing procedure was followed, in accordance with the ASTM E1169-20, "Standard Practice for Conducting Ruggedness Test". Six factors (i.e., air void, strain level, clamp tightness, temperature, frequency, and placement of central clamp) were selected to identify and control the source of variability in the test procedure. Overall, this test method possesses great potential to be considered as a routine fatigue cracking test. The method does not require cutting, gluing or on-specimen instrumentation. As a result, sample preparation and testing times of the 3PBC test method are shorter than typical fatigue tests (e.g., four-point bending and uniaxial fatigue) and the fixture is easy to operate and inexpensive. Therefore, this product will help state agencies or consulting companies to evaluate asphalt mixture characterization while minimizing both costs and the time required.

INTRODUCTION

Fatigue cracking is a critical mode of distress in asphalt pavements. The need for assessing the fatigue characteristics of asphalt concrete was first acknowledged by Hveem (*1*) in 1950s. Proper mix design, structural design, and enhanced material selection can significantly slow down the fatigue cracking and extend pavement service life. To better evaluate the resistance of asphalt pavements to fatigue cracking, numerous laboratory tests have been developed. The most common cracking tests include:

- Flexural Tests (Center Point and Third-Point Loading Tests, Cantilever Beam Rotating Test, Trapezoidal Cantilever Beam Test, and Four-point Bending (4PB) Fatigue Test)
- Supported Flexure (Supported beams (with springs, oil chamber, rectangular rubber, elastic foundation) and supported disk (elastic foundation))
- Uniaxial Fatigue (Direct Tension and Tension/Compression Tests)
- Diametral Tests (e.g., Indirect Tensile Test)
- Triaxial Tests
- Wheel-tracking Tests
- Fracture Tests (e.g., Semi-Circular Bending (SCB-Jc, I-FIT, etc.), Disk-Shaped Compact Tension (DCT) Test)
- Texas Overlay Tester

Among all the tests listed above, the four-point bending (4PB) fatigue test (AASHTO T321) has traditionally been the most common test method to characterize the fatigue resistance of asphalt mixtures. However, 4PB tests are lengthy, cumbersome, and expensive. Extensive material requirement for sample preparation, difficulty in meeting target air void, many samples needed for testing, and excessive equipment cost are some of the challenges encountered when running 4PB tests. As an alternative, uniaxial fatigue (UF) tests (AASHTO TP107 and TP133) have been gaining wide acceptance for fatigue evaluation of asphalt pavements because of their advantages over the 4PB and other tests listed above. These advantages include homogenous stress-strain distribution through the sample, samples being produced using the Gyratory compactor and straightforward application of the constitutive models, such as the Viscoelastic Continuum Damage (VECD) theory. Nevertheless, there are also challenges with the UF testing. For example, the two ends of the sample need to be cut perfectly parallel, and the gluing end-platens using a gluing jig can be cumbersome, and time-consuming. Sometimes 'end-failures' are experienced when sample ends are not cut parallel, or gluing is not done properly. Since the samples are expected to fail in the center, many of the samples and the test results are discarded, leading to excessive sample preparation time and the consumption of material. Furthermore, while the UF testing is superior to 4PB testing, it is currently not suitable as a routine testing alternative for balanced and performance-based mix design approaches. This is because UF testing (sample preparation and testing) takes too much time for a mix design process, which is currently based on quick volumetric testing (e.g., bulk specific gravity, air voids etc.). On the other hand, there are several 'quick' tests for hierarchical classification of cracking susceptibility of asphalt mixtures (e.g., SCB at Intermediate Temperature (SCB-Jc) (ASTM D8044), Illinois Flexibility Index Test (I-FIT), Texas Overlay Test (OT) (Tex 248-F), etc.). While empirical formulations were proposed to calibrate fatigue models in Pavement ME using these tests, mechanistically rigorous formulations do not exist for those tests. Hence, there is a need for a test which addresses not only the challenges listed above but is also simple, sensitive to asphalt mix design, repeatable and practical.

The objectives of this project are: (i) to develop a more practical fatigue testing alternative, (ii) validate the applicability of the Timoshenko beam and Viscoelastic Continuum Damage (VECD) theories in analyzing the data, and (iii) perform ruggedness evaluation of the test. A new and robust testing protocol, herein called the Three-Point Bending Cylinder (3PBC) test has been proposed and discussed in this report. To accomplish these research objectives, multiple tasks were formulated. This report is arranged in such a way so that each task can be addressed and described.

DEVELOPMENT OF 3PBC TEST FIXTURE (TASK 1)

The objective of this part of the study was to improve the design of the 3PBC fatigue testing system. Factors including production cost, ease of use and compatibility with different testing units were considered during the design process. FIGURE 1 illustrates the latest Three-Point Bending Cylinder (3PBC) test setup. This test fixture is composed of a solid base, two fixed end supports used to clamp the sample and a central clamp for application of cyclic (zero-mean) vertical load. Supports and loading clamps are composed of two C-shaped pieces, which are screwed together to hold the asphalt sample in-place. The lower C-shaped pieces are connected (screwed or welded) to the base plate. The distance between the two supports is 125 mm (4.9”) and the inner diameters of clamps are 68 mm (2.7”) each. The base plate includes four orienting knobs to provide proper placement of the central clamp to ensure that the load is applied at the center of the specimen.

The tests in this study were conducted using a servo-hydraulic Material Testing System (MTS) unit as presented in FIGURE 1. The testing temperature in MTS was controlled through a forced-air draft conditioning chamber. A sinusoidal strain-controlled vertical load (with zero mean) is applied at the center of the specimen through the vertically free-moving clamp. FIGURE 2 shows a general schematic view of the 3PBC test setup with proper dimensions. The displacement measurements required for calculating the maximum strain at the bottom-center (or top-center) of the specimen were obtained using two linear variable displacement transducers (LVDTs) attached on both sides of the central clamp. The difference between the two LVDTs was observed to be very low. However, during the test, the strain level was controlled through the actuator strain gauge and not LVDTs. This was done to avoid equipment damage due to the potential instabilities of the actuator caused by the slow feedback of LVDT measurements. This problem is less pronounced in most of the Asphalt Mixture Performance Testers (AMPT), therefore, on-specimen LVDT controlled testing is quite possible with the AMPTs. Besides, a third LVDT was attached to the top of the fixed supports to measure any potential lateral displacement due to steel bending, which is not desirable. As mentioned earlier, the 3PBC is a zero-mean cyclic displacement-controlled test and the test ends when the microcracks propagate through the entire sample diameter (which can be observed visually). The stresses and strains for each cycle were computed using the Timoshenko beam theory.

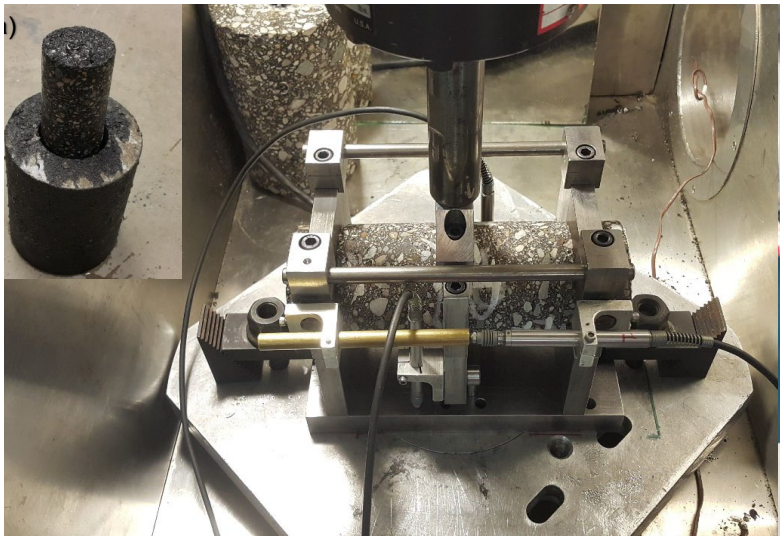

FIGURE 1 3PBC test setup with a loaded specimen in the Material Testing System

ENHANCING THE DESIGN OF THE 3PBC TEST FIXTURE (TASK 2)

SHAFT UPGRADE

As part of Task 2, the research team worked on several ways of improving the 3PBC testing fixture so that the speed of sample mounting is improved, the fixture itself is more robust and it is compatible with a typical Asphalt Mixture Performance Tester (AMPT) equipment, e.g., AMPT by IPC Global. The initial design of the fixture limited the movement of the 3PBC test fixture inside the Asphalt Mixture Performance Tester (AMPT) chamber once the specimen was loaded. Prior to test initiation, a contact load was applied to set the specimen at position zero. However, due to machine compliance and AMPT user program limitations, many times the contact load was high enough to induce damage to the specimen. Another concern was the speed of mounting of asphalt sample into the fixture, which is important to reduce temperature equilibration time. To address these concerns, a new shaft connector was designed and built to connect the central clamp of the 3PBC setup to the top platen of the AMPT. The new system allows mounting of the sample into the AMPT without any danger of applying bending moment during sample placement as shown in FIGURE 3.

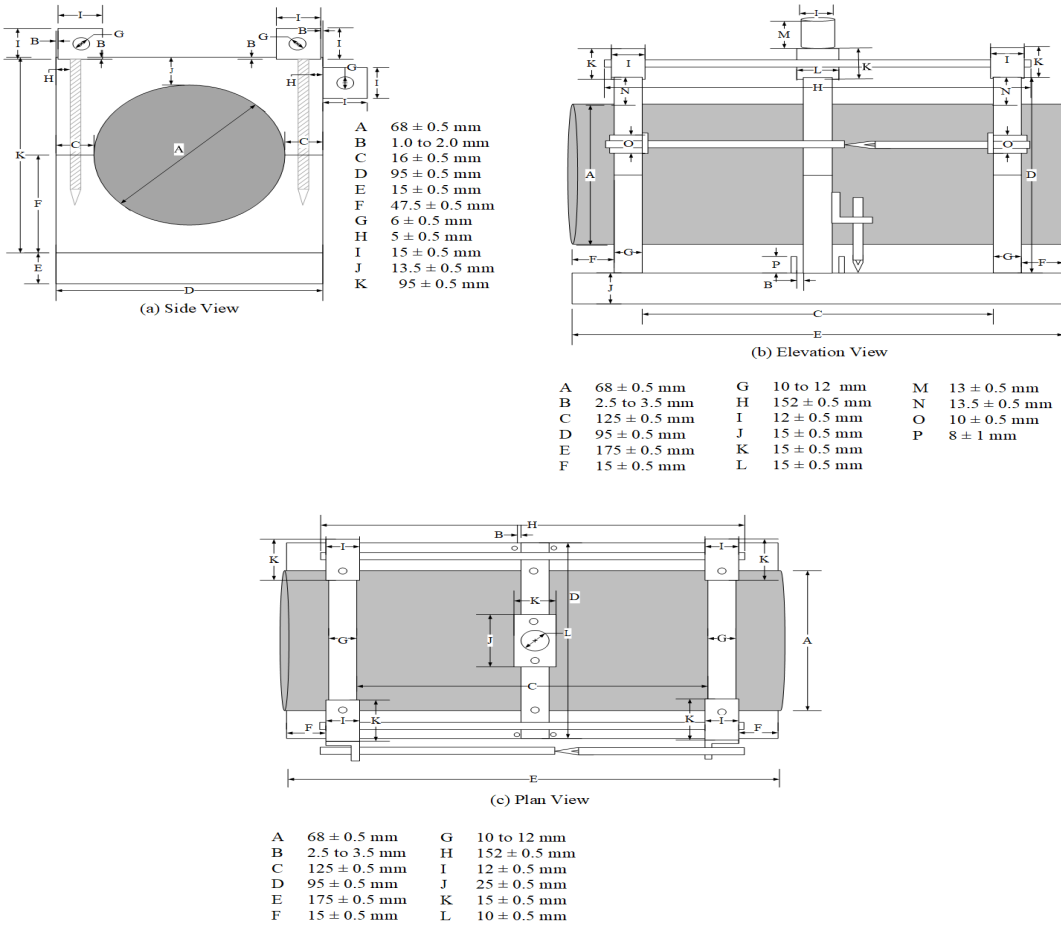

FIGURE 2 General schematic view of the three-point bending cylinder test setup with a loaded specimen: (a) Side View; (b) Elevation View; and (c) Plan View.

SIDE AND CENTER CLAMP UPGRADE

A concern was the potential bending of the 3PBC setup while loading due to fatigue of the steel used to make the side clamps. Bending of side clamps in 3PBC setup affects the assumption of fixed supports on

the sides and results are affected. A new AISI type O1 oil-hardening steel was selected to produce a new 3PBC setup. The O1 steel is a general-purpose non-deforming low alloy for applications requiring extreme dimensional accuracy. It is relatively inexpensive and produced following ASTM A681 − 08. More details regarding the properties of this material are shown in TABLE 1. With the new setup made with AISI type O1 oil-hardening steel, the possibility of any potential bending of the fixture during sample test is minimized. Also, a circular pocket was added to the bottom plate to ensure the fixture aligns at the center of the AMPT actuator.

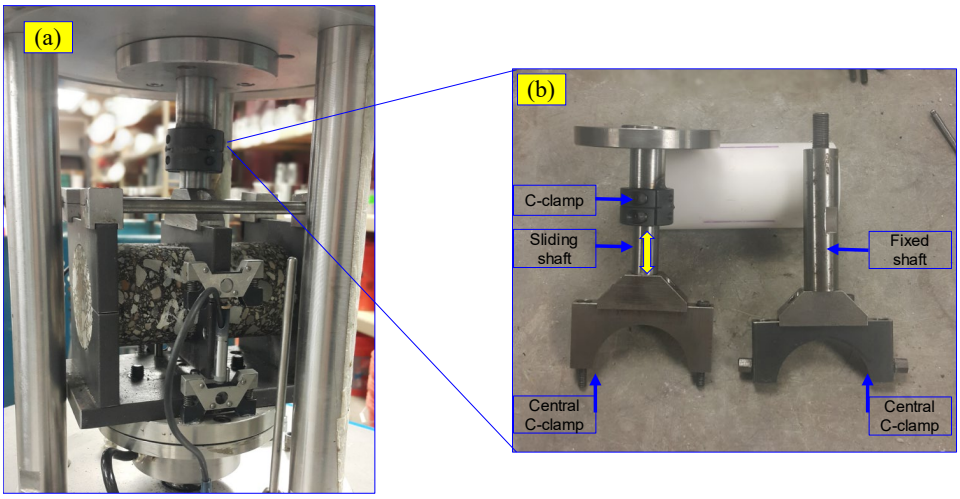

FIGURE 3 (a) 3PBC test loaded specimen and (b) fixed shaft (old design) and sliding shaft (new design) to connect the central clamp of the 3PBC setup to the top platen of the AMPT.

TABLE 1 Physical Properties of The AISI Type O1 Steel

Physical properties	Metric	English
Density	7.83 g/cc	0.283 lb/in³
Modulus of Elasticity	214 GPa	31000 ksi
Poisson's Ratio	0.30	0.30
Shear Modulus	82.0 GPa	11900 ksi

AMPT USER-PROGRAMMABLE SOFTWARE CONFIGURATION FOR 3PBC TEST

In order to run the 3PBC test in AMPT, a new testing protocol was programmed in the AMPT user-programmable software. In this protocol, the Timoshenko beam formulations were implemented. A snapshot of the loading program editor and the main screen of the user programmable testing protocol for the 3PBC are shown in FIGURE 4 and FIGURE 5, respectively. However, this software was not used in this project, other than few runs to test the system. In the next phase of the project, the AMPT will be used with other improvements, for example, non-contact strain measurement methodology to measure the strains on asphalt specimens using an image processing technique. This practice will allow accelerating the 3PBC testing even faster by avoiding the time taken to attach LVDTs.

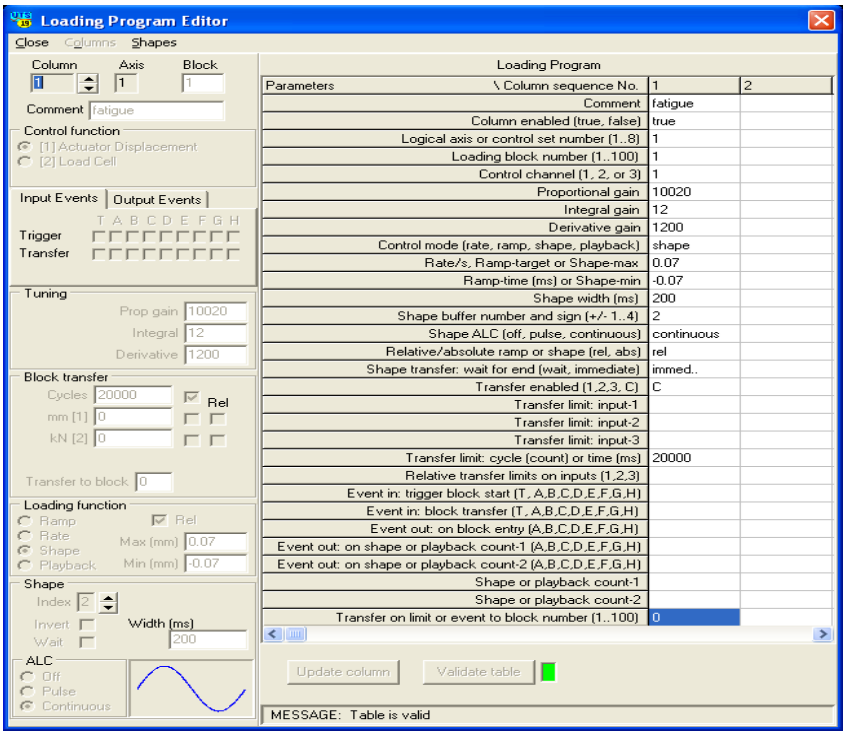

FIGURE 4 AMPT loading program editor.

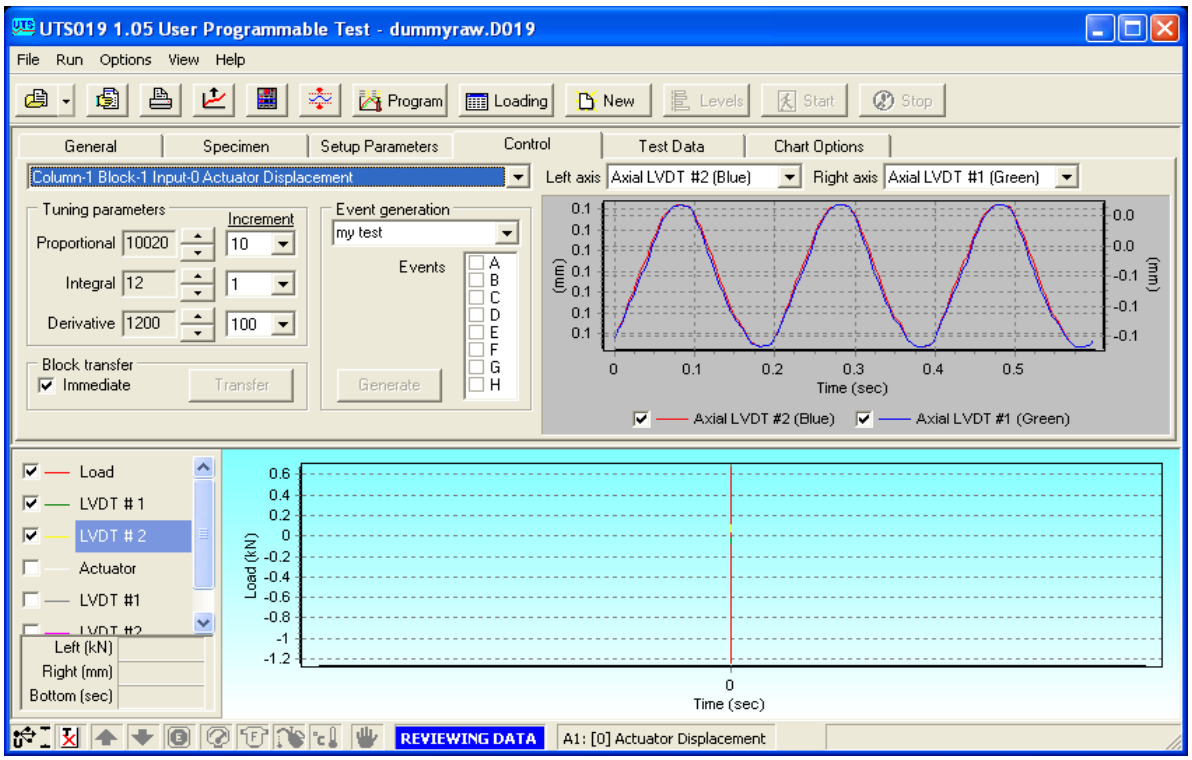

FIGURE 5 Main screen of the user programmable testing protocol for the 3PBC.

VALIDATION OF TIMOSHENKO-EHRENFEST BEAM THEORY FORMULATIONS (TASK 3)

The Euler beam theory commonly used for the analysis of slender isotropic beams considers the beam kinematics in terms of flexural stiffness. The low aspect ratio of 3PBC requires considerations of shear-induced deformations in the so-called "thick-beam", i.e., Timoshenko beam theory (*2,3*).

The analytical formulations presented herein for the stiffness of thick 3PBC are based on the following assumptions:

- The 3PBC is considered as a short beam with both ends clamped
- The central clamp restrains the sample from bending and moves parallel to end-clamps
- Poisson's ratio of 3PBC is assumed to be constant at a given cycle, during a particular test at a certain frequency/temperature combination

TIMOSHENKO-EHRENFEST BEAM MODEL

Initially, the Timoshenko beam theory has been presented herein by considering 3PBC as a linear elastic material. The formulations are then extended to viscoelastic behavior (for a given frequency/temperature combination) using the elastic-viscoelastic correspondence principle (*4*). For a linear elastic, isotropic homogenous slender beam with both ends fixed and loaded at the center by a force P_z, the Euler theory states that the maximum vertical deflection (δ_z) can be calculated as follows (*5*):

$$\delta_z = \frac{P_z L^3}{192 E I_{xx}} \quad [1]$$

where, δ_z is the maximum vertical deflection, L is the span length, E is Young's modulus and I_{xx} is the moment of inertia along axis xx. The schematic view of a fixed beam with a central load is illustrated in FIGURE 6.When the aspect ratio (length to diameter ratio) of a cylindrical beam is less than 6, the shear-induced deflection becomes significant and Euler theory does not apply (*6*). For such beams, Timoshenko beam theory needs to be used to calculate the deflection as follows (3);

$$\delta_z = \frac{P_z L^3}{192 E I_{xx}} + \frac{2\beta P_z L(1+\nu)}{EA} \quad [2]$$

where, β is the shear coefficient, A is the cross-sectional area. Hutchinson (*7*) derived the following expression for the shear coefficient (β) for beams with low aspect ratio:

$$\beta = \frac{6(1+\nu)^2}{7+12\nu+4\nu^2} \quad [3]$$

where, ν is the Poisson's ratio.

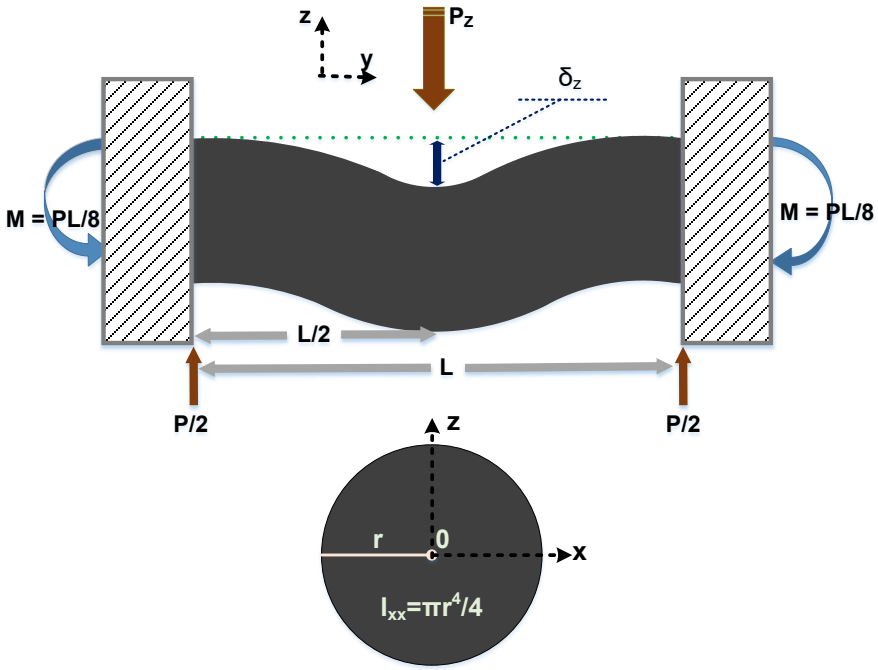

FIGURE 6 Exaggerated deflection of a fixed beam with a central load.

Equation 2 can be rearranged to yield elastic modulus as a function of the vertical load (P_z) and measured deflection at the center (δ_z):

$$E = \frac{P_z L[AL^2 + 384\beta I_{xx}(1+\nu)]}{192\delta_z I_{xx} A} \quad [4]$$

For viscoelastic materials that are exposed to cyclic load at a constant frequency, Equation 4 can be used to calculate the magnitude of the dynamic modulus at each cycle N (i.e., $|E^*|_N$) as follows:

$$|E^*|_N = K\frac{P_z(N)}{\delta_z(N)} \quad [5]$$

$$\mathrm{K} = \frac{\mathrm{L}[\mathrm{AL}^2 + 384\beta\mathrm{I}_{xx}(1+\nu)]}{192\mathrm{I}_{xx}\mathrm{A}} \quad [6]$$

where, $|E^*|_N$ is the (damaged or undamaged) dynamic modulus at each cycle N, $P_z(N)$ and $\delta_z(N)$ are the peak-to-peak load and deflection, respectively.

As part of this task, three-dimensional (3D) Finite Element (FE) analyses were performed to validate the theoretical results obtained from the application of the Timoshenko theory. The 3D FE analyses were performed to simulate the 3PBC test, using the exact geometry of the 3PBC sample and the fixture. Cyclic displacement controlled 3PBC test simulations were performed to compute response on the vertical force in the shaft for a given dynamic modulus level for each element. Then Timoshenko formulations were used to compare and verify the computed dynamic modulus (from Timoshenko beam formulations) and that was used in the 3D FE model. The FEA runs included both 'elastic' and 'viscoelastic' runs. FIGURE 7 shows a view of the FE mesh used. The simulations were run for two intermediate temperatures: 10 ºC and 20 ºC at the following frequencies: 10 Hz, 1 Hz, and 0.1 Hz. In the 'elastic' runs, a constant modulus was assumed

(based on a frequency/temperature combination of the target |E*| being simulated). It is worth noting that the viscoelastic materials (e.g., asphalt mixtures) can be treated as elastic materials when subjected to a cyclic zero-mean test with constant frequency. This practice is theoretically valid when the peak-to-peak results (i.e., force, displacement) are used. In 'viscoelastic' runs, the Prony series coefficients of the asphalt mixtures were obtained from the measured |E*| test and used as input in the ABAQUS. TABLE 2 shows relaxation times (τi) and dimensionless elastic coefficients (gi) of the generalized Maxwell model (Prony series) at 10°C and 20°C for the considered three mixtures in this task.

TABLE 2 Prony series coefficients for the considered asphalt mixtures at 10°C and 20°C

Mix ID	4E30SBS		4E3SBS		4E3DVR	
T (ºC)	10	20	10	20	10	20
G_o (Pa)	8.74E+09	9.40E+09	8.37E+09	8.89E+09	1.18E+10	8.98E+09
τ_i (s)	gi		gi		gi	
1.00E-07	0.0361	0.1013	0.0732	0.1624	0.0931	0.1169
1.70E-06	0.0443	0.1058	0.0716	0.1333	0.0881	0.1095
2.80E-05	0.0887	0.1709	0.1132	0.1706	0.1324	0.1608
4.60E-04	0.1532	0.2137	0.1528	0.177	0.1666	0.1902
7.70E-03	0.2212	0.2013	0.1823	0.157	0.1836	0.1839
1.30E-01	0.2282	0.1275	0.1752	0.1086	0.1605	0.1311
2.20E+00	0.1463	0.0535	0.1263	0.0566	0.1022	0.0669
3.60E+01	0.0569	0.0171	0.0663	0.0229	0.0467	0.0262
6.00E+02	0.015	0.0047	0.0246	0.0077	0.0156	0.0084
1.00E+04	0.0094	0.0036	0.0139	0.0032	0.0107	0.0055

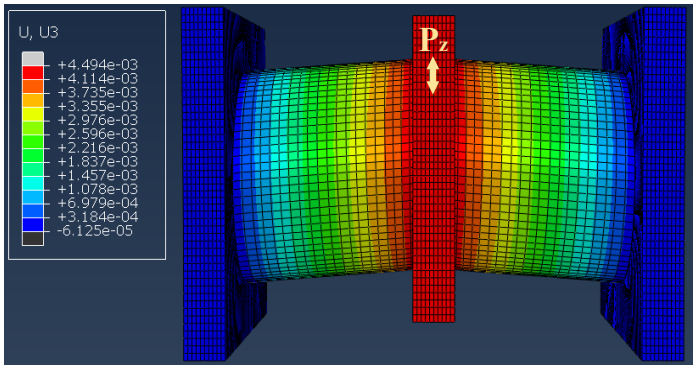

FIGURE 7 Deformation of the 3PBC test sample simulated in 3D FEM (ABAQUS) (Deformation scale factor = 1000).

FIGURE 8 illustrates the input |E*|, which were obtained from the measured master curve (i.e., $|E^*|_{AMPT}$) and the corresponding |E*| (i.e., $|E^*|_{3PBC}$) calculated after ABAQUS simulations using Timoshenko beam theory for different simulations run at different frequencies and temperatures. As shown in FIGURE 8 both the computed elastic |E*| as well as the viscoelastic |E*| values match very well with the values obtained from $|E^*|_{AMPT}$ master curve. While the error in computed elastic |E*| ranges from 0.2 % to 16 %, the error computed for viscoelastic |E*| is less than 12 %. The change in error range between the two simulation modes is primarily related to the assigned material properties and their effects on the mechanical response of the asphalt mixture when subjected to loading. The results also indicate that typically, the error increases with the decrease in loading frequency. However, at high frequency (i.e., 10 Hz), the error for both elastic and viscoelastic simulations is smaller than 5% which is very low considering all the errors that can emanate

from sample preparation. Therefore, the 3PBC tests are recommended to be performed at a frequency of 5 Hz and above, where the maximum error is smaller compared to lower frequencies. Overall, this part of the study showed the applicability of the Timoshenko beam theory to analyze data obtained from the 3PBC tests.

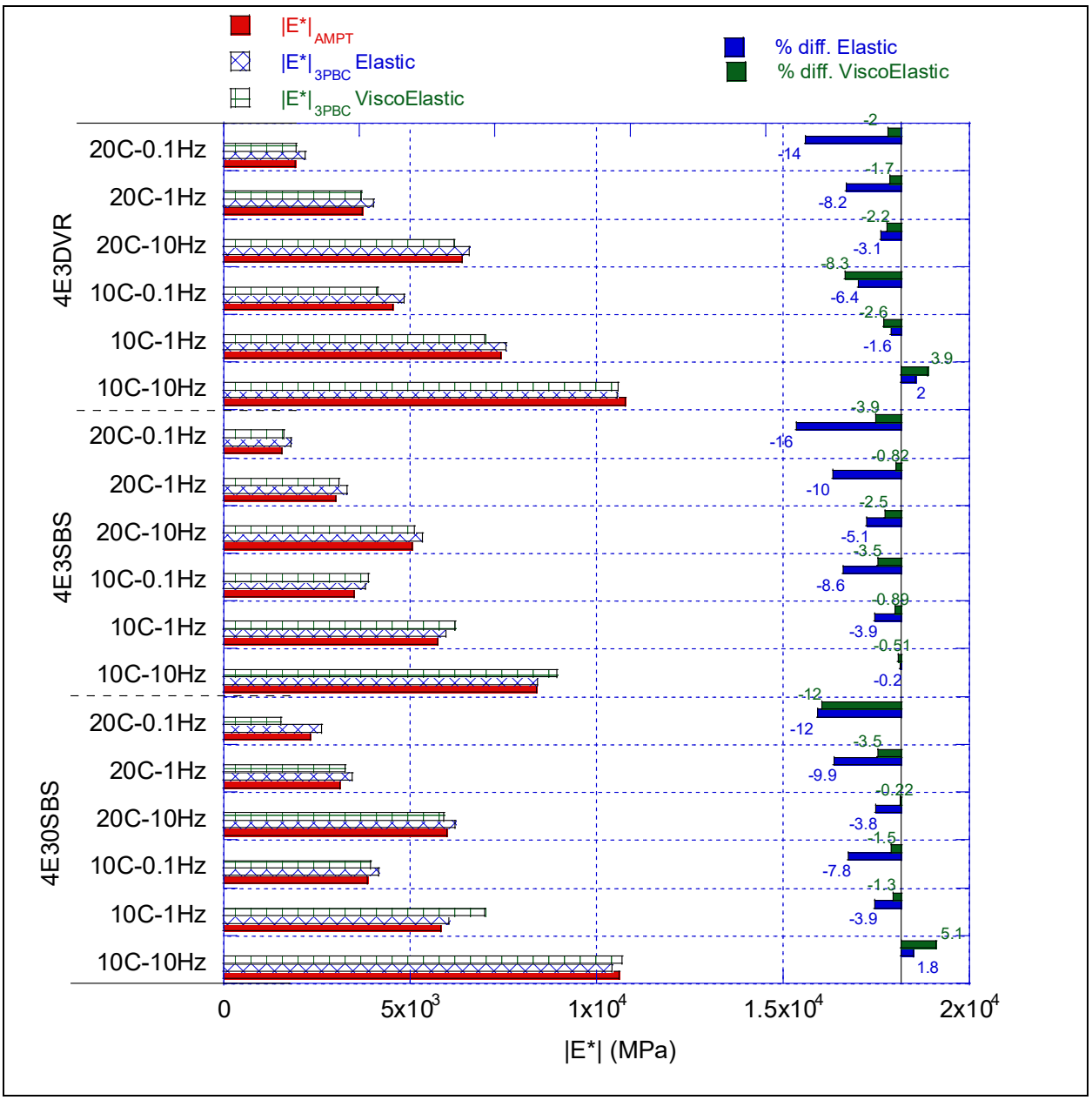

FIGURE 8 Comparison of |E*| values input to 3D FEM and those computed by the Timoshenko beam theory in elastic and viscoelastic modes.

LITERATURE ON POISSON'S RATIO

Since Poisson's ratio is an input to the Timoshenko beam formulations used in the 3PBC test, a literature review was conducted to better understand the ranges of Poisson's ratio reported in the literature for asphalt mixtures. The lack of a standard test configuration or measurement procedures limits the available experimental database and direct calculations of this property (*8*) (*9*) (*10*). Furthermore, the published

Poisson's ratio values generally show variability, especially in tests that are carried out at stress and strain levels that exceed the linearity limit (*11*) (*12*). Therefore, Poisson's ratio of asphalt pavements is often not a measured property, rather a default value (i.e., 0.35) is used in pavement design.

Past researchers measured Poisson's ratio using both axial tests on the cylindrical specimen and indirect tension (IDT) testing (*13–17*). The conducted measurements have indicated high dependency of Poisson's ratio values on test configuration (*17*), where magnitudes of Poisson's ratio varied depending on loading mode, test temperature and frequency (*13,18*). While at low temperatures and high frequencies the Poisson's ratio can be as low as 0.06, at high temperatures and low frequencies it approaches to 0.5 (*10,17,19*). In monotonic testing, the Poisson's ratio was measured using three loading modes: tensile relaxation, compressive relaxation, and tensile constant rate strain. Despite the test configuration mode, an increase of Poisson's ratio value in time was revealed (*16,20*). A summary of the reported Poisson's ratio values in the literature is shown in TABLE 3. Although in theory, the Poisson's ratio may be measured using the AASHTO R83 test procedure, this requires precise radial LVDTs, which is not available in the AMPT. The low strain levels are difficult to measure and demand a highly sensitive measuring setup, which in turn can increase the cost of the AMPT.

EFFECT OF POISSON'S RATIO ON THE |E*| COMPUTED FROM 3PBC TEST

Since Poisson's ratio is an input in the 3PBC formulations, typical values reported in the literature were used to investigate the sensitivity of $|E^*|_{3PBC}$ to Poisson's ratio. As part of this task, 3PBC test results for three different mixtures were analyzed. The effect of varying Poisson's ratio values on $|E^*|_{3PBC}$ was investigated. The number of cycles to failure at 50% reduction in $|E^*|_{3PBC}$ initial value was used to compare the fatigue performance of the asphalt specimens.

TABLE 3 A Summary of Reported Poisson's Ratio Values at Intermediate Temperatures

Test configuration	Range of reported Poisson's Ratio at intermediate temperatures	Reference
IDT (cyclic)	0.27 – 0.30	(*17*)
Uniaxial (cyclic)	0.07 – 0.10	
IDT	0.25 – 0.35	(*21*)
Uniaxial (cyclic)	0.15 – 0.32	(*18*)
IDT (relaxation)	0.18 – 0.22	(*16*)
IDT (cyclic)	0.22 – 0.38	
IDT (cyclic)	~ 0.25	(*13,22*)
Uniaxial (tensile relaxation)	0.27 – 0.45	(*20*)
Uniaxial (compression relaxation)	0.23 – 0.27	
Uniaxial (tension/compression)	0.25 – 0.32	(*15,23*)

The results of one of the asphalt samples tested are shown in FIGURE 9. The sample was subjected to a sinusoidal loading at 10ºC and 5Hz in strain controlled (actuator displacement control) mode. The initial microstrain level was 200, which slightly increased and then stayed constant until failure. Timoshenko beam theory formulations were used to calculate the reduction in stiffness at each cycle. The reduction in stiffness (i.e., |E*|3PBC) for each loading cycle was calculated using several Poisson's ratio values within the range of 0.10-0.40.

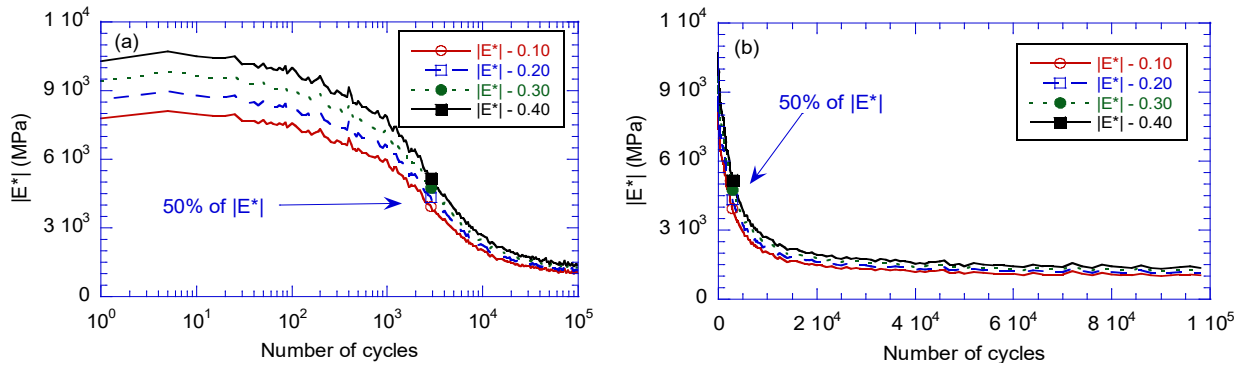

FIGURE 9 Evolution of $|E^*|_{3PBC}$ using different Poisson's ratio values for loading cycle.

The results presented in FIGURE 9 show that the $|E^*|_{3PBC}$ increases with the increasing Poisson's ratio. As shown, although |E*| versus cycles graphs shift up or down due to the magnitude of the Poisson's ratio, the calculated N_f does not change. Since N_f is the main outcome of the test, it can be suggested that a constant value of 0.3 can be used as an average to compute the N_f.

EVALUATION OF APPLICABILITY OF VISCOELASTIC CONTINUUM DAMAGE THEORY (VECD) TO THE 3PBC TEST RESULTS (TASK 4)

Adaptation of VECD theory in fatigue characterization of asphalt mixtures significantly reduced the experimental burden required to calibrate phenomenological fatigue life formulation (i.e., $N_f = a\varepsilon^{-b}E^{-c}$). The VECD constitutive model is based on Schapery's proposed elastic-viscoelastic correspondence (E-VC) principle, which can be applied to both linear and non-linear viscoelastic materials, and work potential theory. The E-VC principle states that the constitutive equations for a particular viscoelastic media are equivalent to equations of elastic media when the concept of pseudostrain is used instead of actual physical strain (*24*). The primary strength of this approach is the so-called damage characteristic curve (C-S) which is a unique curve that can be used to predict the fatigue life of asphalt mixtures at different frequencies and temperatures at a required strain level (*25*). The C-S curve is computed from the peak-to-peak stress-strain data retrieved for each cycle.

One of the prerequisite steps of the VECD-based characterization is the determination of the linear viscoelastic |E*| master curve. Therefore, |E*| test needs to be run for analysis of 3PBC test results. In this part of the study, a 3E3 (19 mm NMAS base course designed to maximum traffic of 3 million ESALs) plant produced lab compacted mixture was selected. The job mix formula of the selected mixture included a PG58-28 binder. FIGURE 10 illustrates the |E*| master curves in log scale and semi-log scale for each mixture, respectively. The damage characteristic (C-S) curves were constructed for each replicate of the 3PBC test run at various temperatures and frequency combinations. According to the VECD theory, C-S curves computed from the data of each replicate should collapse to form a unique curve.

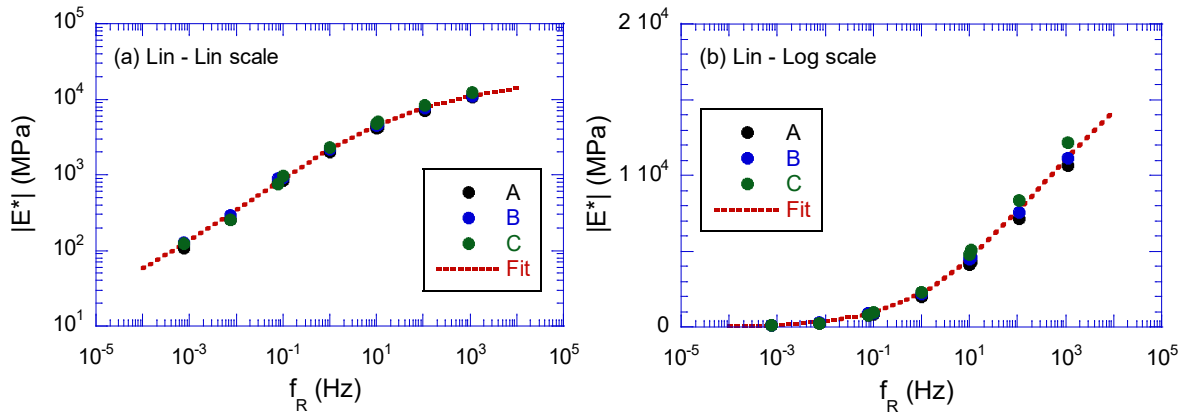

FIGURE 10 Linear viscoelastic properties of the mixtures: (a) log-log scale and (b) semi-log scale plots of dynamic modulus master curve for 3E3 asphalt mixture.

The C-S curves of the 3E3 mixture for the 3PBC test are shown in FIGURE 11. Despite the large aggregate size (19 NMAS), which is a crucial factor affecting the continuum medium, the C-S curves collapsed to form a single curve (with slight variations due to sample-to-sample variability) regardless of strain level, temperature, and frequencies. The C-S curve of the first replicate tested at 20ºC, however, followed a different trend compared to other replicates. The data obtained from this sample are excluded from further consideration due to abnormal behavior of the C-S curve, tied to different factors including but not limited to the sample preparation.

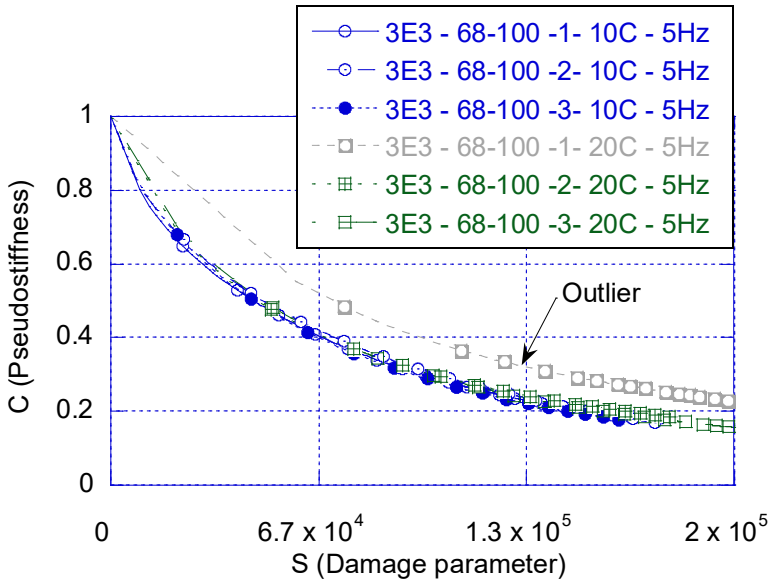

FIGURE 11 Damage characteristic curves of 3PBC tests run on 3E3 (19mm) mixture.

DEVELOPMENT OF VECD SOFTWARE FOR THE 3PBC TEST

In order to facilitate the analysis of 3PBC data using the VECD theory, a software program was developed. The beta version of the software is called 3PBC-VECD. A screenshot of the software is shown in FIGURE 12. A user tutorial of the 3PBC-VECD software program has also been drafted and included in Appendix D. A few features of the software are listed below:

- Once the laboratory uniaxial dynamic modulus (|E*|) data is entered, the software generates the |E*| master curve, converts the |E*| master curve to creep compliance (E(t)) and automatically computes the maximum slope (α) of the logE(t)-log(t) graph. The parameter alpha (α) as well as the |E*| master curve coefficients are inputs to the VECD-based analysis in later steps.
- The 3PBC data obtained from a typical Material Testing System (MTS) output can directly be loaded to the software as a csv file. Also, multiple samples can be loaded at the same time. Alternatively, the 3PBC data can also be 'copied' and 'pasted' into an input table in the second step of the program.
- All sample data loaded can be visualized by using various plotting options.
- The VECD damage characteristic curve (i.e., C (pseudo stiffness) vs S (damage parameter) curve) is automatically generated by the program for each sample.
- Software calculates number of cycles to failure (N_f) at different temperatures/frequencies, for each sample by simulating a perfect strain-controlled fatigue test (using the C vs S curve established earlier).
- Software automatically fits the traditional fatigue life equation used in MEPDG and generates the 'Beta' values. These 'Beta' values can be used in Pavement ME as well as MEAPA software.

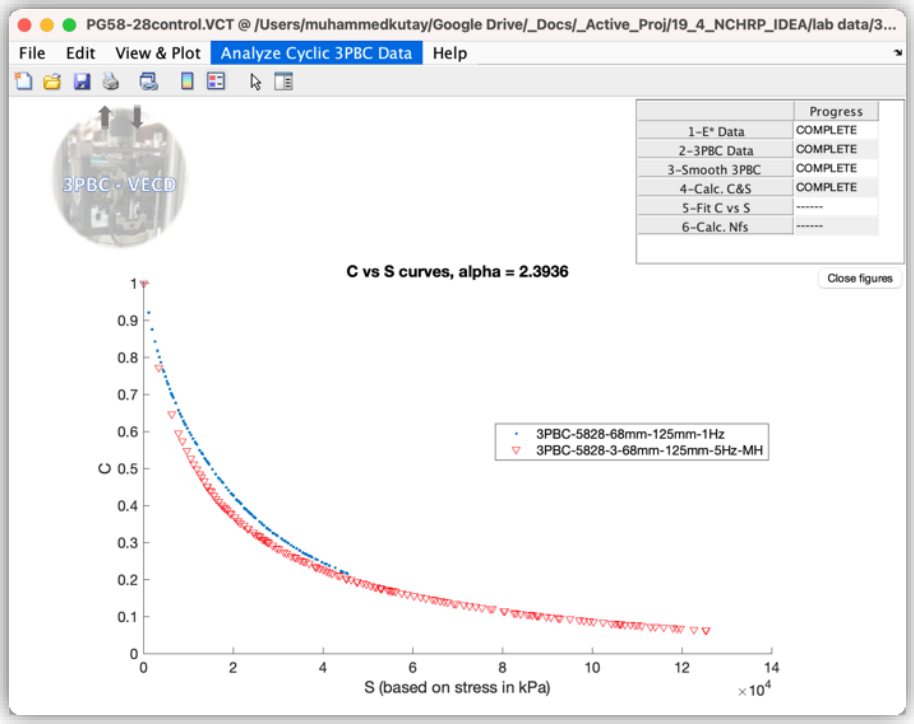

FIGURE 12 A screenshot of the newly developed 3PBC-VECD software.

POISSON'S RATIO MEASUREMENTS DURING FATIGUE TESTS (TASK 5)

In this task, additional push-pull tests were performed on three different types of asphalt mixtures to measure the Poisson's ratio during the uniaxial fatigue test. Then these values were used as input during the 3PBC test analysis and initial (during the first cycle) 3PBC moduli were compared to those obtained from the uniaxial |E*| master curve. The three mixtures were all 4E3 mix (12.5 mm NMAS leveling course designed to maximum traffic of 3 million ESALs), and they were obtained from a construction site located in Okemos, Michigan. The first mixture was made with an unmodified PG58-28 binder. The second mixture was made with a PG70-28 styrene-butadiene-styrene (SBS) polymer modified. Finally, the third mixture was made with a PG58-28 binder, but the mixture included polymer coated rubber (PCR), added as a 'dry'

process at the asphalt plant. In this task, the objective was to capture the effect of different binder types on the Poisson ratio of a sample during a fatigue test, because fatigue behavior of mixtures is more significantly affected by the binder characteristics rather than aggregate structure at intermediate temperatures. Later parts of this study include 3PBC fatigue test run on different aggregate size/gradations where the effect of aggregate skeleton is evaluated.

DYNAMIC MODULUS TEST

As part of VECD modeling, dynamic modulus tests were also performed on these mixtures. Field-collected loose mixtures were compacted in lab using the Superpave gyratory compactor to 180 mm. Then 4" diameter and 6" tall samples were prepared by cutting and coring gyratory compactor specimens. Samples were prepared such that 7±0.5% air void was maintained. These samples (3 replicates for each mixture) were tested in uniaxial compression mode at different temperatures (4°C, 20°C, and 40°C) and loading frequencies (25, 10, 5, 1.0, 0.5, and 0.1 Hz). FIGURE 13(a) through FIGURE 13(c) illustrates the |E*| master curves in log scale for each mixture and FIGURE 13 (d) shows comparative |E*| master curves in log scale for three mixtures. As observed, SBS modified PG70-28 mixture had the highest stiffness among the other two asphalt mixtures. The control PG58-28 and PCR PG58-28 mixtures exhibited almost identical |E*| master curves.

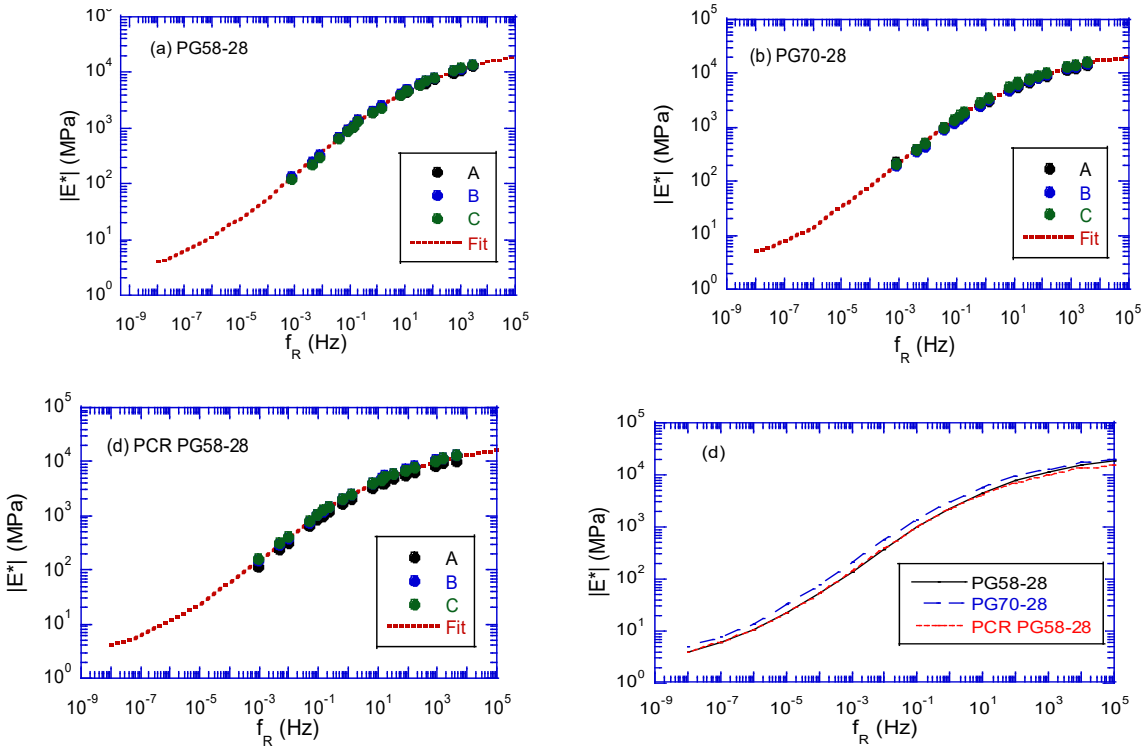

FIGURE 13 Linear viscoelastic properties of the mixtures. In the figure, f_R = reduced frequency and |E*| = dynamic modulus.

POISSON'S RATIO MEASUREMENTS

During uniaxial push-pull fatigue tests, Poisson's ratio (ν) was measured by using a radial LVDT (a chain and loose core LVDT combination) and two axial LVDTs as shown in FIGURE 14. It is to be noted that two axial LVDTs were mounted at 180° apart from each other. A servo-hydraulic Material Testing System (MTS) unit was used to conduct push-pull tests at actuator displacement-controlled mode for two different

temperatures, i.e., 10°C and 20°C at 5 Hz frequency. At each temperature, two samples from each individual mixture were tested. The target on-specimen strain level was set as 250 microstrain at the beginning of the test. It should be noted that since the tests were actuator displacement control mode, on-specimen strain increased during the test. This does not pose a problem because the VECD model can be calibrated using any random peak-stress/ peak-strain combination during a fatigue test. Once the VECD model is calibrated (i.e., the C vs S curve is obtained), perfect strain-controlled tests can be simulated with the VECD model at any strain/frequency and temperature combination. During these subsequent simulations, the failure criterion for the push-pull test was set as a 50% reduction in the initial modulus. A push-pull test sample was 130 mm in height and 68 mm in diameter.

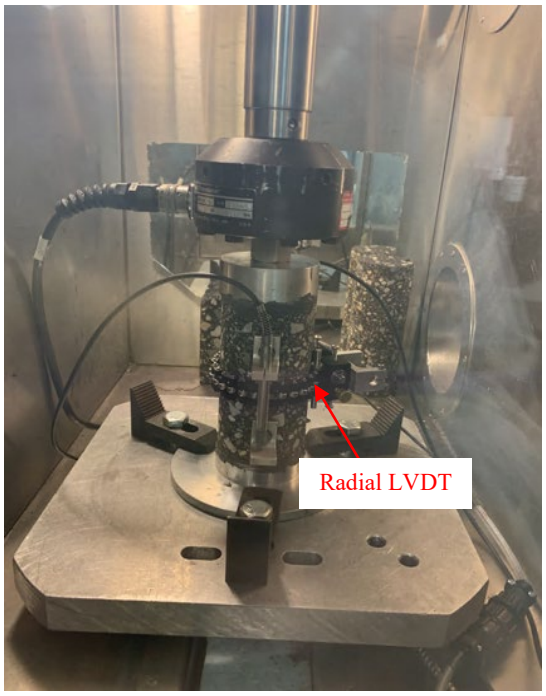

FIGURE 14 Poisson's ratio measurement setup in MTS.

Poisson's ratio (ν) results are shown in FIGURE 15 (a) through FIGURE 15 (c) for PG58-28, PG70-28, and PCR PG58-28, respectively. The first observation from the figures is that the Poisson's ratio did not significantly change during the fatigue test, although a slight decrease was observed in some mixtures at specific temperatures. Previous research showed that the Poisson's ratio is inversely proportional to the |E*| (*18*). However, it appears this is correct for 'intact' samples. During the fatigue test, although |E*| decreases due to the damage, the Poisson's ratio does not increase. As a result, it can be inferred that the Poisson's ratio and |E*| cannot be correlated during a fatigue test. The second observation from FIGURE 15 (a)-(c) is that, in general, the Poisson's ratio is lower at 10°C as compared to 20°C, which is consistent with the literature, whereas |E*| increases with decreasing temperature for intact samples, Poisson's ratio decreases (*16,18*). Although Poisson's ratio measurements vary depending on loading mode, test temperature and frequency, results show that modifications in asphalt binder type did not affect the measured ν significantly. This also supports previous literature (*17*). Based on these results, an average value of 0.3 for Poisson's ratio can be recommended to be used in 3PBC tests. However, further experimental verification is necessary to identify factors affecting Poisson's ratio measurement. For example, mixtures with one binder type and three different aggregate sizes or types can be evaluated.

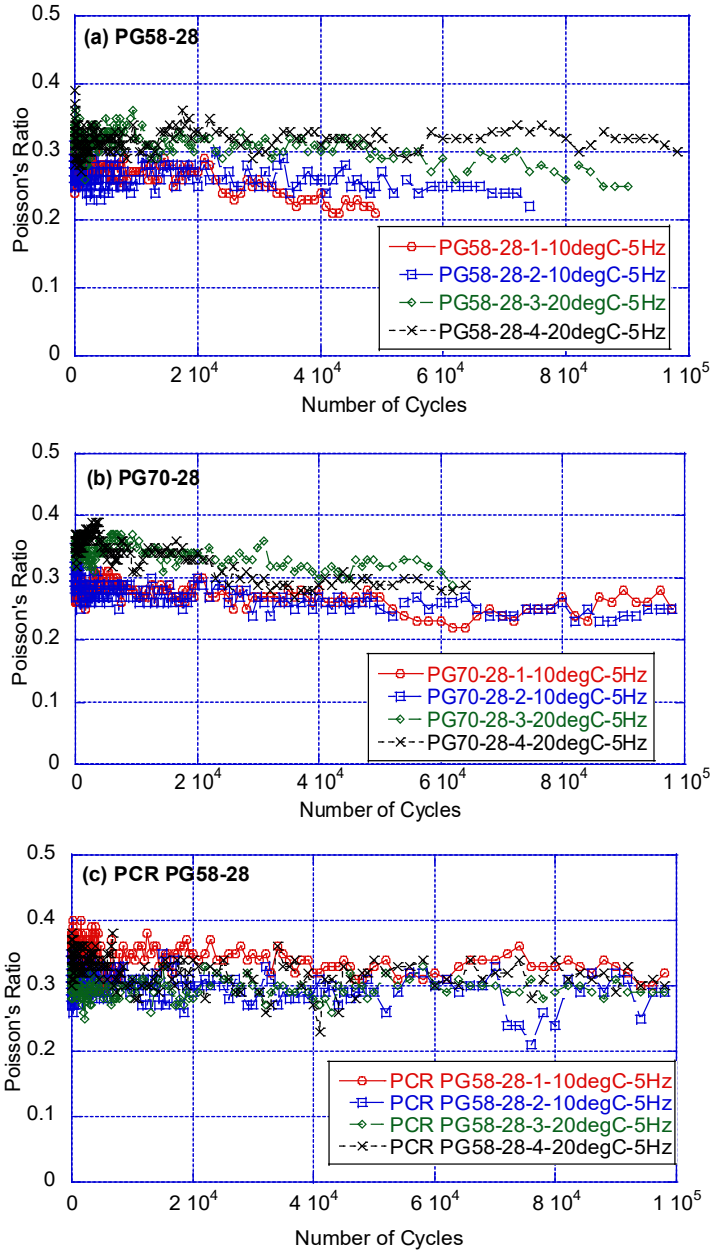

FIGURE 15 Evolution of Poisson's ratio during the push-pull fatigue tests for mixtures: (a) PG58-28 (b) PG70-28 and (c) PCR PG58-28.

The average Poisson's ratio values for each type of mixture are presented in TABLE 4. At a particular temperature (10°C or 20°C), average Poisson's ratio for two replicates is similar. However, PCR samples show some variability as it contains crumb rubber which might influence the Poisson's ratio. Also, due to lack of PCR loose mixtures, additional push-pull tests could not be conducted. TABLE 4. also presents the coefficient of variance (COV) for each replicate which is less than 10%.

TABLE 4 Summary Results of Measured Poisson's Ratio

Mixture	Specimen ID	Test Temperature (°C)	Average Poisson's Ratio	Standard Deviation	COV
PG58-28	1	10	0.272	0.022	8%
	2	10	0.265	0.016	6%
	3	20	0.313	0.021	7%
	4	20	0.317	0.017	5%
PG70-28	1	10	0.277	0.018	6%
	2	10	0.278	0.022	8%
	3	20	0.341	0.016	5%
	4	20	0.342	0.029	8%
PCR PG58-28	1	10	0.348	0.021	6%
	2	10	0.303	0.022	7%
	3	20	0.296	0.016	5%
	4	20	0.327	0.024	7%

The Poisson's ratio values measured during the push-pull tests were used to analyze the 3PBC fatigue data. First, the initial moduli values were compared against the linear viscoelastic |E*| values obtained from the uniaxial |E*| master curve data. The ratio of initial |E*| from the fatigue test and the |E*| from the uniaxial data is defined as the 'I' value, which is used in the VECD formulations. The I value should theoretically be equal to unity. However, due to the sample-to-sample variability, gluing effects in the Push-Pull tests, clamping effects in 3PBC test, the 'I' value typically varies from 0.7 to 1.4.

FIGURE 16 shows the variation of the 'I' value in both Push-Pull and the 3PBC tests at 10°C and 20°C. As shown, 'I' values from 3PBC tests are found to be closer to unity than those obtained from the Push-Pull tests. This supports that 3PBC fatigue test performance is equivalent or in some extent better than Push-Pull test. Also, it can be observed, in both tests, the variation of I value is reasonable, which further validates the Timoshenko-Ehrenfest Beam Theory formulations used in analyzing the 3PBC test.

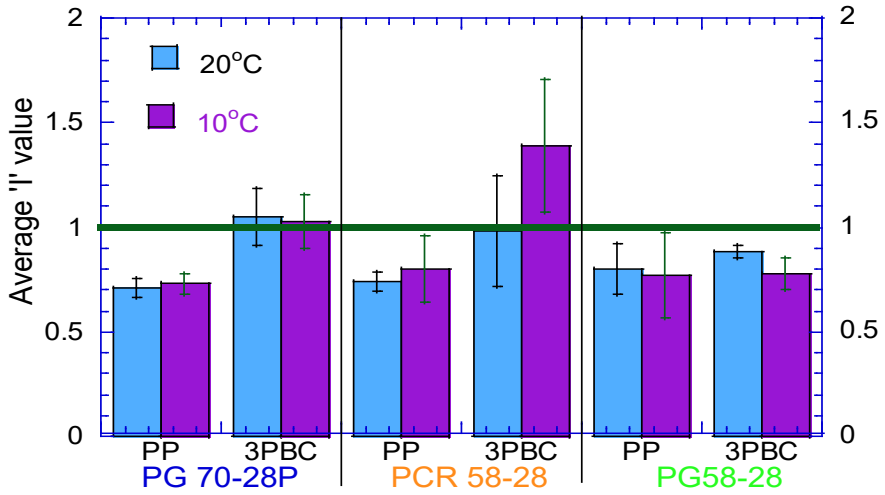

FIGURE 16 Summary "I" values for three mixtures at both 10°C and 20°C.

RUGGEDNESS EVALUATION (TASK 6)

According to NCHRP 9-29 report (*26*), test methods are expected to provide accurate results when the sources of variability are controlled. Ruggedness evaluation is the appropriate method to identify important sources of variability by intentionally varying the most influential parameters. Such examination provides evidence on the reliability of the test technique during ordinary usage and helps establish control thresholds. Hence, ruggedness testing is a crucial part of the development of a new test method and as such, was performed in this study.

In this study, two sets of ruggedness testing were performed. Initially, a preliminary ruggedness evaluation was performed (herein called Phase I ruggedness) to study air voids and geometrical factors. Later in Phase II, more factors were investigated, by following the ASTM E1169-20, "*Standard Practice for Conducting Ruggedness Test*"*(27*). ASTM E1169 provides a practical procedure for concurrently evaluating the effects of certain changes in each of the operating conditions in an independent manner. This practice recommends that ruggedness testing should involve a single laboratory on uniform material and potentially followed up by an inter-laboratory (round-robin) study. The inter-laboratory study was not within the scope of this work, but it should be considered in a future study.

PHASE I EXPERIMENTS

Material Properties

The asphalt mixture used for the Phase I was obtained as a loose mix from a local asphalt plant in Lansing, MI. A 5E3 neat (unmodified) mixture was used in this phase. It is noted that 5E3 is a Michigan DOT designation that means that this is a "5E" mixture, which is a 9.5 mm NMAS surface mix, designed to withstand 3 million ESALs, per Superpave mix design requirements. The mix design and volumetric properties of the loose mixture are shown in TABLE 5. The loose 5E3 mix was carefully sampled in 5-gallon metallic pails to avoid segregation. Usually, from a 5-gallon metallic pail, three Superpave Gyratory Compactor (SGC) specimens can be prepared. Prior to loose mixture separation, the 5-gallon metallic pail was reheated at 110 ºC until the loose mix is easily spreadable. This process usually takes less than 3 hours. The loose mixture was poured into a metallic pan and mixed to provide homogeneity. Then, three smaller pans were filled with the required mass of the specimen and placed in a preheated oven at the compaction temperature. To minimize the aging of the loose mix, the temperature of the material was frequently checked using thermocouples. Then the material was poured into compaction molds and an SGC Pine compactor was used to compact the specimen at a specific height to meet required target air voids. Before any further mechanical processing, the compacted samples were stored to cool down at room temperature overnight. All the SGC samples were compacted at a height of 180 mm and a diameter of 150 mm. Depending on the performance test, cylindrical samples were cored and cut at desired diameters and heights. Subsequently, the physical properties of the resized specimens were measured and recorded. The specimens falling out of the predefined air void range were discarded from further testing.

TABLE 5 The Properties of the 5E3 Asphalt Mixture

Mixture ID	5E3
Mix Design ESALs (Millions)	3
Binder content by weight (%)	6.3
Binder PG	PG64-28
NMAS (mm)	9.5
Design air void content (%)	3.5
Voids in Mineral Aggregate, VMA (%)	16.4
Voids Filled with Asphalt, VFA (%)	78.7
Recycled Asphalt Pavement, RAP (%)	22

Factors and Levels of Ruggedness Analysis

The factors and their levels considered for the Phase I ruggedness study are presented in TABLE 6. In this table, the initial geometry of the 3PBC test setup herein is referred to as reference geometry. As previously mentioned, the air void sensitivity for each combination was investigated. It is worth noting that all test samples were cored in a vertical direction.

TABLE 6 Factors and Corresponding Levels for the Ruggedness Evaluation of 3PBC Test

Factors	Reference geometry	1st	2nd	3rd	4th
Air Voids (%)	6, 7, 8	6, 7, 8	6, 7, 8	6, 7, 8	6, 7, 8
SGC specimen height (mm)	180	180	180	180	180
Test specimen diameter (mm)	68	68	38	38	100
Span length (mm)	125	135	100	125	135
Coring Direction	Vertical	Vertical	Vertical	Vertical	Vertical
Test temperature	15	15	15	15	15
Test frequency (Hz)	5	5	5	5	5
Strain (με)	150	150	150	150	150

The 3PBC tests were performed using a closed-loop servo-hydraulic material testing system (MTS) containing an environmental chamber. FIGURE 17 illustrates the test setups and cored test specimens for the 38mm and 100mm diameter samples. The reference 68 mm diameter sample is not shown here for brevity (see FIGURE 2). As shown in FIGURE 17a, for 38 mm diameter samples, the 3PBC test setup components were kept the same as the reference setup designed for 68 mm samples. For 100 mm diameter samples, as shown in FIGURE 17b, the thickness of the base plate and side claps were increased. This was mainly done to avoid any undesired deformation of the fixed ends which could influence the test results. Prior to testing, the temperature of the test specimens was checked using a dummy specimen of the same size as the |E*| samples with a thermocouple inside. During the 3PBC tests, the displacement level at the actuator was initially selected through a trial-and-error process to ensure the on-specimen LVDT measurements showed the strain level on the sample was about 200 microstrains (με). The frequency of the 3PBC tests was 5 Hz, and the tests were conducted at a temperature of 15ºC. The testing conditions were kept the same for all the test combinations. Viscoelastic Continuum Damage (VECD) theory was then used to analyze the data from the 3PBC test results. This allowed the determination of fatigue life (N_f) at target strain levels (i.e., 150 and 300 με for this part of the study), the temperature of 15 ºC and frequency of 5 Hz.

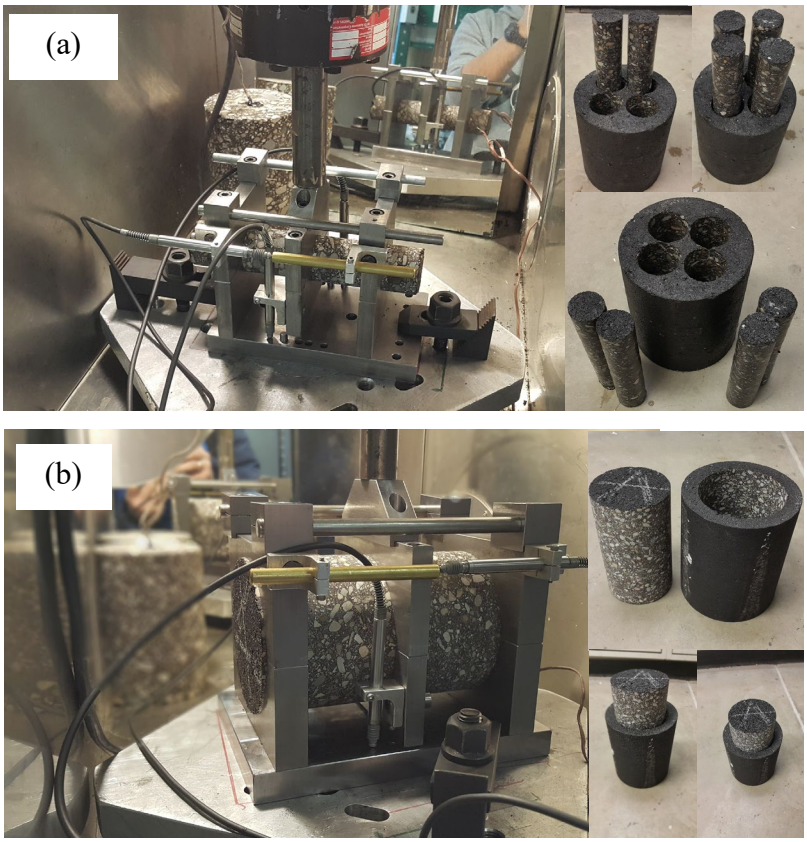

FIGURE 17 The 3PBC test setup with loaded specimens in the Material Testing System (MTS) with a diameter of (a) 38 mm and (b) 100 mm.

Uniaxial Dynamic Modulus (|E*|) Test

Samples for uniaxial dynamic modulus (|E*|) were obtained from cylindrical samples (150 mm diameter, 180 mm height) compacted with the Superpave Gyratory Compactor (SGC) in general accordance with the AASHTO R83 protocol. Cores were extracted from those samples using a diamond-coring stand, while the ends of the cores were trimmed using a masonry saw in order to obtain smooth and parallel end surfaces. The final height of the testing samples was set to 150 mm in all cases. The diameters of the cored samples were 100 mm. The mass of the mixture compacted by the SGC was determined to reach the target air voids content of 7 % ± 0.5 % at the sample core. At least two replicates for each test and mix were prepared. The |E*| measurements were carried out in accordance with the AASHTO R84 protocol using the Asphalt Mixture Performance Testing (AMPT) device. Samples were subjected to uniaxial sinusoidal compressive stress at four temperatures (4, 20, 40 and 54 °C) and three frequencies (10, 1, and 0.1 Hz) at each temperature. The dynamic modulus master curve was obtained using the time-temperature superposition (TTS) principle (*28*) (*29,30*). The dynamic modulus master curve was obtained at a reference temperature (T_{ref}) of 21°C by shifting the |E*| values horizontally. The amount of shift is different at each temperature and defined by the so-called shift factor coefficients a(T). The following second-order polynomial equation can be used to develop the relationship between shift factors and the corresponding temperature:

$$\log\left(a_T\left(T\right)\right) = a_1\left(T^2 - T_{ref}^2\right) + a_2\left(T - T_{ref}\right) \quad [7]$$

where, T_{ref} is the reference temperature (chosen by the user), T is temperature, a_1 and a_2 are the polynomial fit coefficients for the temperature shift factor. During the shifting process, shift factors vary until a good fit to the |E*| data at all the temperatures are obtained using the following sigmoidal function:

$$\log\left(\left|E^*\right|\right) = b_1 + \frac{b_2}{1+\exp\left(-b_3 - b_4 \log\left(f_R\right)\right)} \quad [8]$$

where, b_1, b_2, b_3, and b_4 are the sigmoid coefficients and f_R is the reduced frequency, which is the product of frequency (f) and the shift factor coefficient (i.e., $f_R = f^*a(T)$). FIGURE 18a and b illustrate the |E*| master curves of the 5E3 mixture in log scale and semi-log scale for each replicate. Also, the relationship between the shift factors and the temperature is shown in FIGURE 18c. The |E*| master curve and shift factor coefficients are provided in TABLE 7.

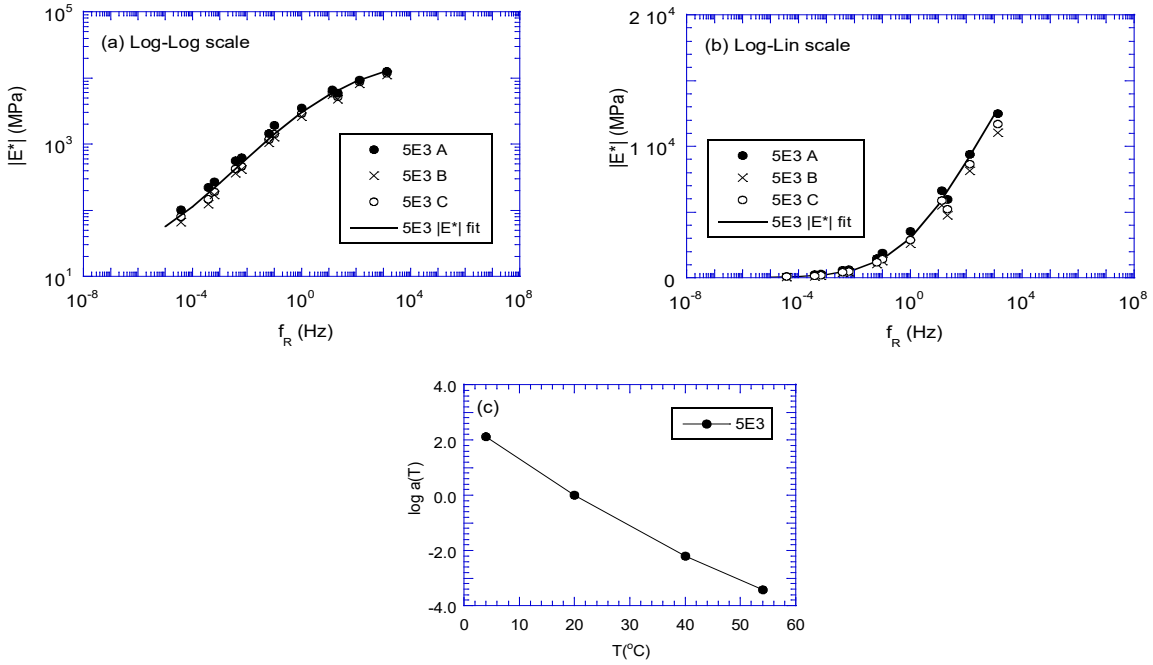

FIGURE 18 Linear viscoelastic properties in (a) log-log scale, (b) semi-log scale plots of dynamic modulus master curves and (c) shift factor coefficients as a function of temperature for 5E3 mixture.

TABLE 7 Dynamic modulus master curve and shift factor coefficients for 5E3 mixture

Coefficient Title	Coefficient Values
Shift factor (a(T)) coefficients:	a1=0.0006, a2=-0.1478
Sigmoidal coefficients:	c1=0.9344, c2=3.4658, c3=1.0157, c4=0.4397

Analysis of 3PBC test results

Effect of Air Void Content

The effect of air void content on fatigue performance of the mixtures is important, as demonstrated in several studies (*31,32*). Close control of this parameter is a crucial task. The current state of practice addresses ± 0.5 % air void tolerance. A wider tolerance range would be helpful to optimize the specimen

preparation time and resources. Generally, the required field air void content is 7 % and used in this study as control air void content for the tested mixtures. While several trial samples for each combination were used to ensure the on-specimen strain level is close to 200 microstrains, the lateral LVDT was used to measure the lateral displacement of the side clamps. FIGURE 19 shows that the lateral displacement is less than 10 % of the vertical displacement except for two cases for 6 % air void content. Since the lateral displacement at 7 % and 8 %, air void contents were below 10 % of the vertical displacement, the lateral displacement limit was set at 10 % of the vertical displacement. Further FE analyses should be performed to quantify if the lateral displacement limit of 10 % affects the stress-strain behavior of the loaded specimen.

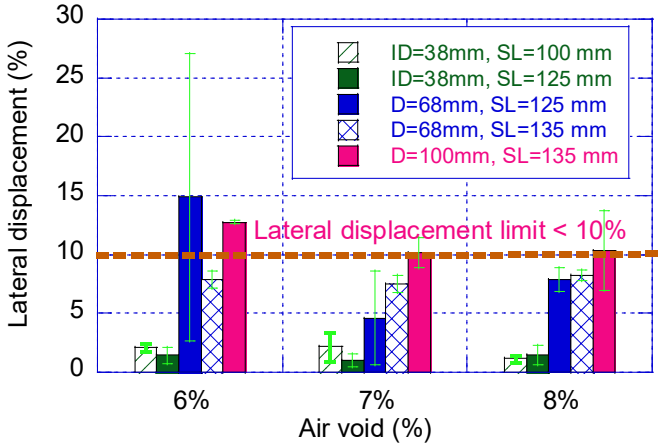

FIGURE 19 Lateral displacement limit for 3PBC test. Vertical axis shows the lateral displacement divided by the vertical displacement in the central clamp, in percentage.

FIGURE 20 Damage characteristic curves for 6 %, 7 % and 8 % air void contents at frequency of 5 Hz, temperature of 15 °C for several testing geometries. FIGURE 20 shows the damage characteristic (i.e., C vs S) curves obtained from specimens tested at 6 %, 7 %, and 8 % air void contents, for different specimen geometries. In all geometries, variability between the individual tests for each air void content is low, as evidenced by the clear collapse of the C (pseudostiffness) versus S (damage parameter) curves. It appears that the effect of air voids on the test 3PBC test results was not significant within the 6-8% air void range.

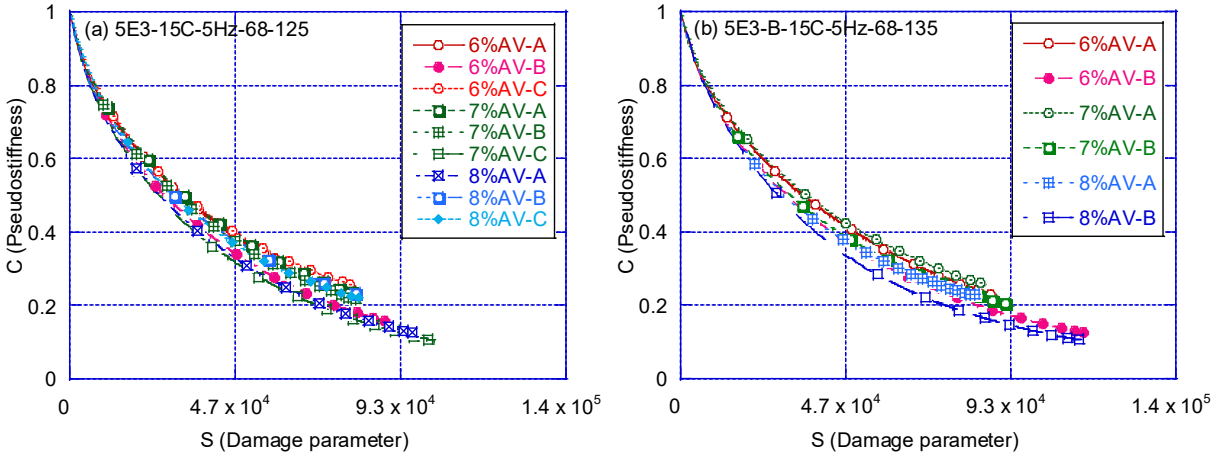

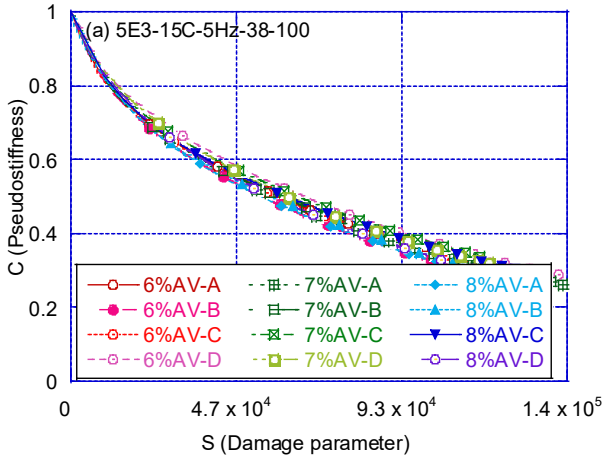

FIGURE 20 Damage characteristic curves for 6 %, 7 % and 8 % air void contents at frequency of 5 Hz, temperature of 15 °C for several testing geometries

Effect of Span Length

Span length is one of the parameters that might affect the stress-strain distribution on the specimen when subjected to loading. This effect becomes more pronounced when the so-called low aspect ratio or "thick-beams" are used, which is the case for the 3PBC test. Different span lengths were adopted and their effect on fatigue life (i.e., N_f) of asphalt mixtures was explored. It is worth noting that from the practical point of view, the span length should be compatible with horizontal coring from field cores (i.e., 150mm diameter cores) or slabs. FIGURE 21 shows the damage characteristic curves (C-S) of all geometries (different span lengths and diameters) and all air void levels. As shown, in general, different span lengths of a given diameter collapsed in a single curve, with slight differences. The N_f values obtained at two different microstrain levels of 150 με and 300 με are presented in a and b, respectively. It appears that in general, the change in span length does not affect the N_f value significantly. The differences are a bit more pronounced for the 38 mm diameter specimens when compared to the 68 mm diameter specimens. This could be because of the higher variability observed in the 38mm diameter, 125 mm long samples. One-way ANOVA was performed to assess the effect of span length for a given diameter on the N_f. The measured N_f values at different air void contents (i.e., 6 %, 7 %, and 8 %) were, however, combined for each geometry, respectively. P-values and Tukey's analysis for each scenario are presented TABLE 8. From the table, it is shown that the effect of span length on N_f is not statistically significant. Overall, the effects of span length on the 3PBC test results are minimal.

Effect of Specimen Diameter

Investigation of the applicability of the 3PBC test to different sample diameters is important because the recommended sample thickness (i.e., 68 mm (2.7")) for the 3PBC test may prevent its use for thin lifts of asphalt mixture layers. FIGURE 21 shows the effect of the diameter on the damage characteristic curves (C-S). As shown, C vs S curves of larger diameter samples are below those of the smaller-diameter samples. shows the number of cycles to failure based on the C versus S curves computed for each diameter. As shown, the N_f values decreased with increasing diameter. The fatigue life for 38 mm diameter 3PBC test samples is higher compared to the reference geometry (68 mm) diameter and the 100 mm diameter has the shortest fatigue life. This trend is consistent in all air void contents and in strain levels (see FIGURE 22a and FIGURE 22b).

TABLE 8 Statistical Evaluation on the Effect of Span Length and Diameter on Fatigue Life of Asphalt Mixture

Geometry combination	P-Value				Grouping+
	d = 68 mm l = 125 mm	d = 68 mm l = 135 mm	d = 38 mm l = 100 mm	d=38 mm l=125 mm	
d = 68 mm l = 125 mm					B\C
d = 68 mm l = 135 mm	1	-			B\C
d = 38 mm l = 100 mm	0.064	0.066	-		A
d = 38 mm l = 125 mm	0.001	0.001	0.379	-	A
d = 100 mm l = 135 mm	1	1	0.043	0.001	C

*N_f is significantly different if P-Value < 0.1; +N_f that do not share a letter are significantly different

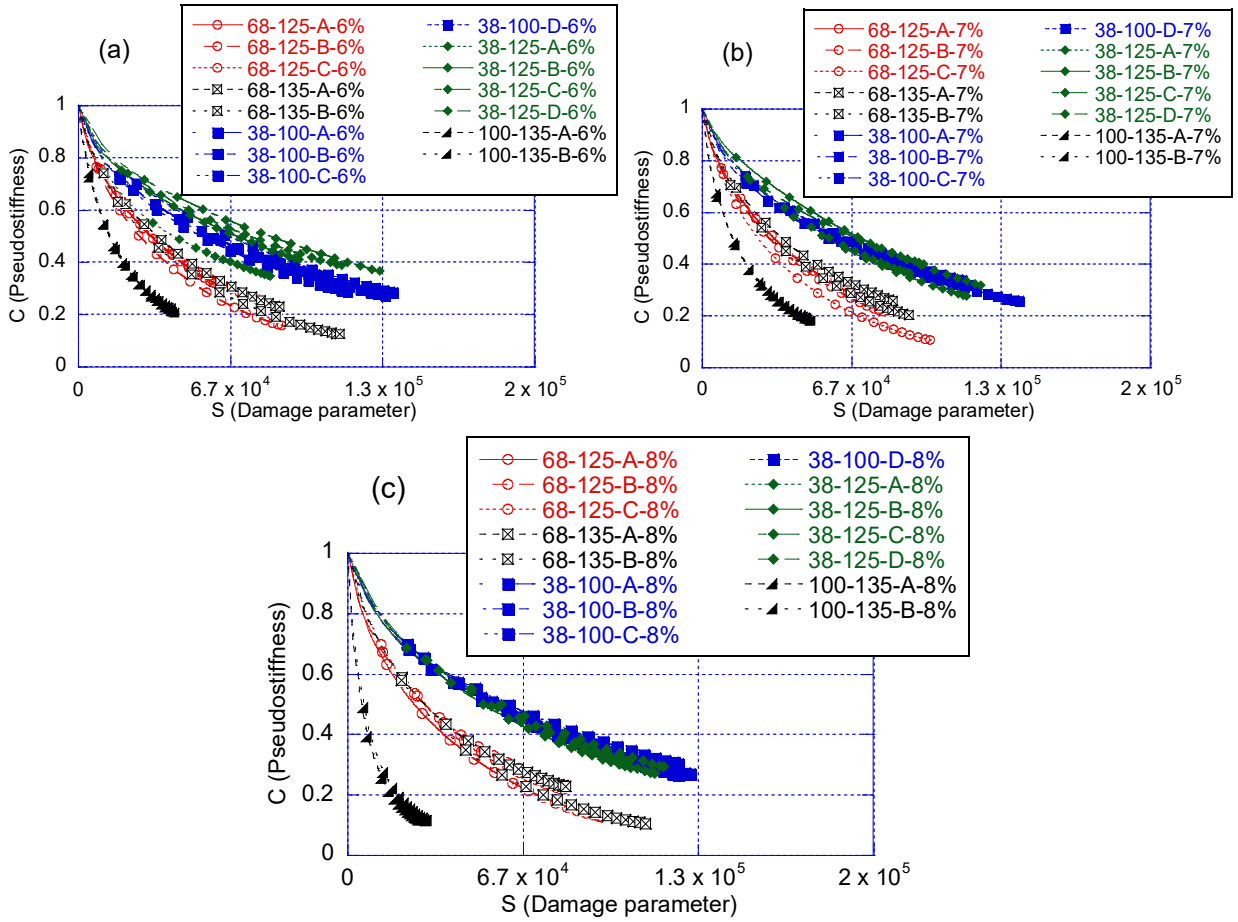

FIGURE 21 Damage characteristic curves (C-S) of all geometries plotted for (a) 6 %, (b) 7 % and (c) 8 % air void contents.

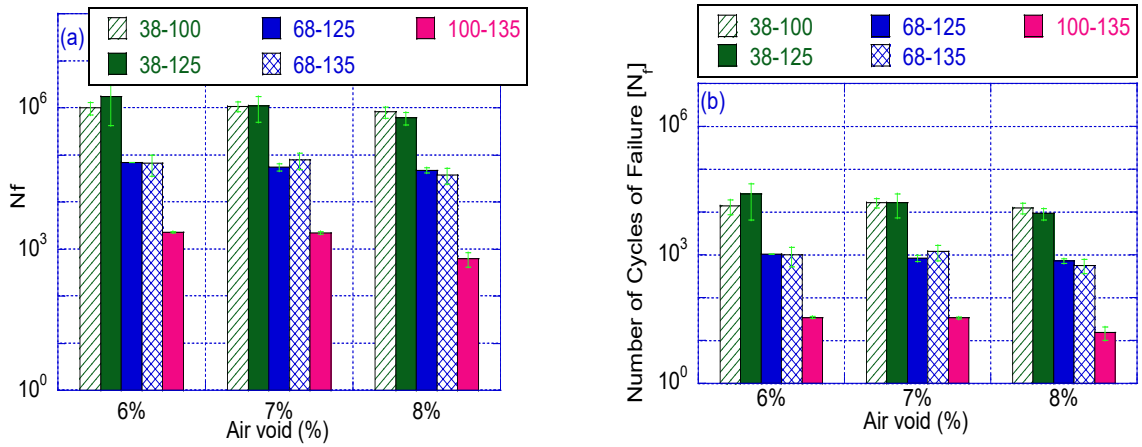

FIGURE 22 Number of cycles to failure (Nf) results for different length and diameter combinations at (a) 150 με and (b) 300 με.

PHASE II EXPERIMENTS

Material Properties

In this phase of the study, an asphalt mixture from a local asphalt plant in Lansing, MI was obtained. The mixture was a 4E3 mixture (12.5 mm NMAS leveling course designed to maximum traffic of 3 million ESALs). A summary of the mixture properties is provided in TABLE 9. This part of the study considered samples of 68 mm in diameter, 180 mm in height (no saw cut was done, only required coring was done from a gyratory compacted sample) and the fixture span length was 125 mm. The sample preparation steps were the same as those mentioned in the first part of the ruggedness study (i.e., Phase I).

TABLE 9 Asphalt Mixture Properties for the 4E3 Mixture

Mixture ID	4E3
Mix Design ESALs (Millions)	3
Binder content by weight (%)	5.40
Binder PG	PG64-22
NMAS (mm)	12.5
Design air void content (%)	4.0
Voids in Mineral Aggregate, VMA (%)	15.5
Voids Filled with Asphalt, VFA (%)	74.2
Recycled Asphalt Pavement, RAP (%)	26.77

Factors and Levels of Ruggedness Analysis

The ruggedness testing plan in the ASTM E1169-20 standard follows the partial factorial Plackett-Burnam design, and it requires seven factors to be selected at two different levels (i.e., low and high). These seven factors are generally selected theoretically or based on prior knowledge or experiences. Selected factors can be quantitative (e.g., time, temperature, etc.) or qualitative (e.g., wet vs dry, open vs close, etc.). The advantage of this partial factorial design is that instead of running too many tests, it requires only a total number of 16 determinations or test runs with two replicate sets for seven factors. In this study, six factors were selected and one factor was repeated to adhere to the above-mentioned requirement of the Plackett-Burnam partial design method (*33*). TABLE 10 shows the selected six factors and their corresponding low- and high-level values. These factors were selected based on the research team's experiences gained so far dealing with the 3PBC test fixture and test data.

TABLE 10 Selected Factors with Two Levels for Ruggedness Testing

Factors	Low Level	High Level
Air Voids	4%	6%
Strain	200 $\mu\epsilon$	400 $\mu\epsilon$
Clamp Tightness	Partial tight (10 lb-in)	Full tight (30 lb-in)
Temperature	10 ℃	20℃
Frequency	5 Hz	10 Hz
Placement of Central Clamp/Eccentricity	0 mm	6 mm

TABLE 11 presents the experimental design for the ruggedness testing with seven factors plus one factor to be repeated to fulfill the seven factors requirement) and eight determinations. In TABLE 11, within the same row of an individual determination number, +1 refers to the higher-level value of a specific factor and -1 refers to the lower-level value of another factor. The Plackett-Burnam partial factorial design is established in such a way that for all the determination numbers (i.e., eight in this case without replicates), each factor must be varied an equal number of times (i.e., four times in this case) at both lower and higher levels. Brief descriptions of the six factors selected in this study are provided below.

Air Void: Air void is one of the important parameters to be measured for asphalt concrete. Air void was selected as a ruggedness factor at relatively lower levels i.e., 4% and 6%. These values were chosen because the team had already studied the effects of the larger air voids (i.e., at 6-8%) at the first part of the ruggedness evaluation.

TABLE 11 Ruggedness Testing Matrix

Determination #	Air Void	Strain Level	Clamp Tightness	Temperature	Frequency	Placement of Central Clamp (Eccentricity)	Air Void
1	1	1	-1	1	-1	-1	1
2	-1	1	1	-1	1	-1	-1
3	-1	1	1	1	-1	1	-1
4	1	-1	1	1	1	-1	1
5	-1	-1	-1	1	1	1	-1
6	1	1	-1	-1	1	1	1
7	1	-1	1	-1	-1	1	1
8	-1	-1	-1	-1	-1	-1	-1

Strain Level: Two different strain levels (i.e., 200 $\mu\epsilon$ and 400 $\mu\epsilon$) were selected. It should be noted that the tests were conducted in 'actuator' displacement control mode in our Material Testing System (MTS) unit. Therefore, the tests were not truly strain controlled. The actuator displacement levels were selected via trial and error such that initial strain levels on the specimen were close to the target strain level (i.e., 200 $\mu\epsilon$ or 400 $\mu\epsilon$). As tests continue, strain levels measured on the specimen increased. This does not pose a problem because the data is analyzed using the Viscoelastic Continuum Damage (VECD) theory and the damage characteristic curves (i.e., the C vs S curves) were calibrated using the data collected. Then the VECD theory is again utilized to simulate a perfectly strain controlled test to obtain the number of cycles to failure (N_f).

Clamp Tightness: Clamp tightness was selected as a ruggedness factor to investigate the effect if/when an operator does not pay proper attention to the side clamp tightness. Two side clamps were tightened at two levels (i.e., fully tight or partially tight). The clamp tightness was quantified by a torque meter with a dialing gauge. Torque levels of 30 lb-in and 10 lb-in were adopted to make the side clamps fully and partially tight, respectively. It is to be noted that the central clamp was tightened as usual in the full tight mode.

Temperature: Typically, the fatigue behavior of asphalt pavement is observed at intermediate temperatures. Bodin et al. *(34)* found that for displacement-controlled fatigue tests, number of cycles to failure of asphalt mixtures was maximum at the temperature range of 10 ℃ to 20℃ . It is also noted that fatigue lives over different temperatures show a parabolic like shape and the least number of cycles to failure varies with mixture types. In this ruggedness test, two temperatures (i.e., 10 ℃ and 20 ℃) were selected to investigate the effect on 3PBC test results.

Frequency: The fatigue behavior of an asphalt mixture also depends on the frequency (or rate of load application). As part of Task 3 of this project, it was found that at 5 Hz and above frequency levels, the initial stiffness of asphalt samples computed by the Timoshenko beam theory matched well with the dynamic modulus of the same mixture tested at the same frequency in the AMPT machine. Therefore, to further investigate the effect of different frequency levels on 3PBC test, two frequency levels (i.e., 5 Hz and 10 Hz) were selected in the ruggedness test.

Placement of Central Clamp/Eccentricity: To investigate the eccentricity effect due to the central clamp's misalignment relative to the middle of the sample span length, the base of the 3PBC fixture in the MTS chamber was shifted by 6 mm (0.25 inches) towards one of the sides. At normal central position, the distance between the edge of the top part of central clamp to the either side of clamp's inner edge was measured as 56 mm. To incorporate the eccentricity effect, the same distance was changed to 50 mm, measured from the central clamp to the nearest side clamp's inner edge.

Dynamic Modulus Tests

As dynamic modulus (|E*|) is a required input needed for analysis of 3PBC data using the Viscoelastic Continuum Damage (VECD) theory, dynamic modulus test was performed before conducting ruggedness test. Dynamic modulus tests were performed and the |E*| master curves were developed in accordance with AASHTO R84 (*35*). Collected loose mixture was compacted at the Advanced Asphalt Characterization Lab (AACL) at MSU using the Superpave gyratory compactor to 180 mm in height. Then 4" diameter and 6" tall samples were prepared by cutting and coring gyratory compactor specimens. According to the ruggedness testing plan, samples were prepared such that 4±0.5% and 6±0.5% air voids were maintained. Prepared samples (3 replicates for each air void percentage) were tested in uniaxial compression mode at different temperatures (4°C, 20°C, and 40°C) and loading frequencies [(10, 1, 0.1 Hz for 4°C, 20°C) and (10, 1, 0.1, 0.01 Hz for 40°C)]. FIGURE 23 shows the |E*| master curves for samples prepared at 4% and 6% air voids. As observed, 4% air void shows slightly higher stiffness at low temperature and high frequency than 6% air void. However, at high temperature and low frequency both these air voids show similar level of stiffness. Dynamic modulus master curve and shift factor coefficients of the PG64-22 at both air voids (i.e., 4% and 6%) are tabulated in TABLE 12.

TABLE 12 Shift Factor Coefficients

Shift Factor (a(T)) Coefficients	PG64-22 (4% air void)	PG64-22 (6% air void)
a_1	0.00052	0.00039
a_2	-0.153	-0.148
Sigmoidal Coefficients		
b_1	0.364	0.412
b_2	4.263	4.185
b_3	1.228	1.171
b_4	0.355	0.351

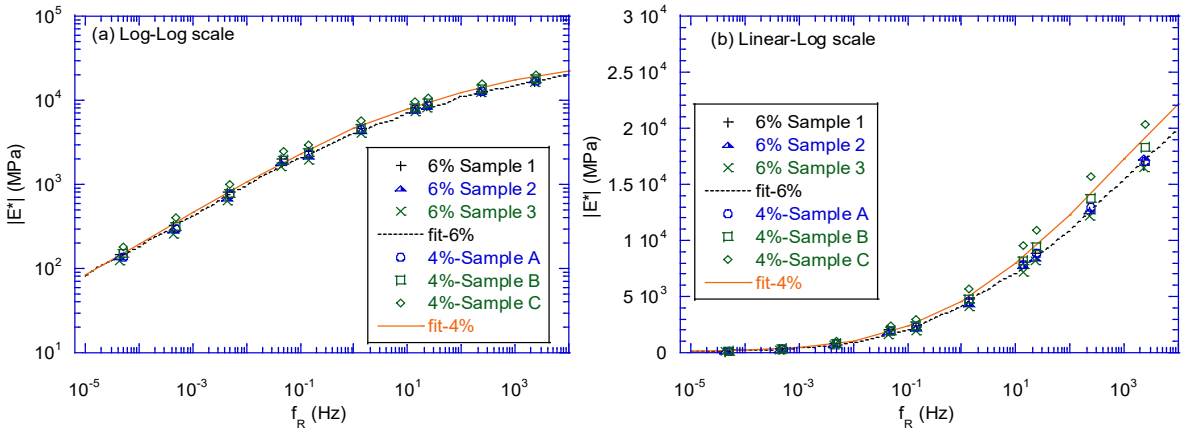

FIGURE 23 Linear viscoelastic properties of the 4E3 PG64-22 mixture: (a) Log-Log scale (to emphasize lower left corner) (b) Linear-log scale (to emphasize upper right corner). Note: f_R = reduced frequency and |E*| = dynamic modulus.

Analysis of 3PBC Ruggedness Tests

The ruggedness evaluation process was started with performing 16 test runs (8 combinations x 2 replicates) with varying low and high levels of the selected factors. The number of cycles to failure, N_f for each of the determination numbers was calculated using the VECD formulations. The C vs S curve represents the reduction in modulus (C) due to the increase in the number of microcracks (S). The 50% reduction in the initial modulus was selected as the failure criterion to calculate the N_f for each determination number with two replicates. FIGURE 24 represents the C vs S curves for all the determination numbers with two replicates.

Following the ASTM E1169-20, statistical analysis of the ruggedness test was conducted in two steps:

- *Main Effect Estimation*: If the factors are independent, the main effect estimation is the best way to represent a factor's influence. The main effect was calculated by subtracting the average response of high level (+1) values from the average response of low-level values (-1). Then main effects are represented as absolute values as shown in TABLE 13.
- *Statistical Significance Analysis:* Once all main effects are calculated for individual factors, statistical analysis was done to identify variable effects using the student's t-test. Student's t-test value was calculated by dividing absolute main effect by standard error of effects ($S_{effects}$). The calculation equations for $S_{effects}$ are represented by Equation 9 and Equation 10. At 0.05 significance level, if the calculated t-value for a factor was greater than the corresponding t-value, the factor would be statistically significant. TABLE 13 and TABLE 14 present all the calculated numbers and FIGURE 25 shows the half-normal plot. A half-normal plot is used to graphically identify potentially statistically significant effects. A reference line in the half-normal plot was drawn with

a slope of 1/se. Potentially significant effects are those that fall farthest to the right of the line. In FIGURE 25, except frequency, all other five factors fall farthest right of the line indicating as significant factors in 3PBC test results.

$$S_{effect} = \sqrt{\frac{4S_{tr}^2}{N \times n}} \quad [9]$$

$$S_{tr} = \frac{S_d}{\sqrt{2}} \quad [10]$$

where, N = number of runs in the design, (N = 8); n = number of replicates, (n = 2); and S_{tr} = the estimated standard deviation of the test results; and S_d = standard deviation of the test results.

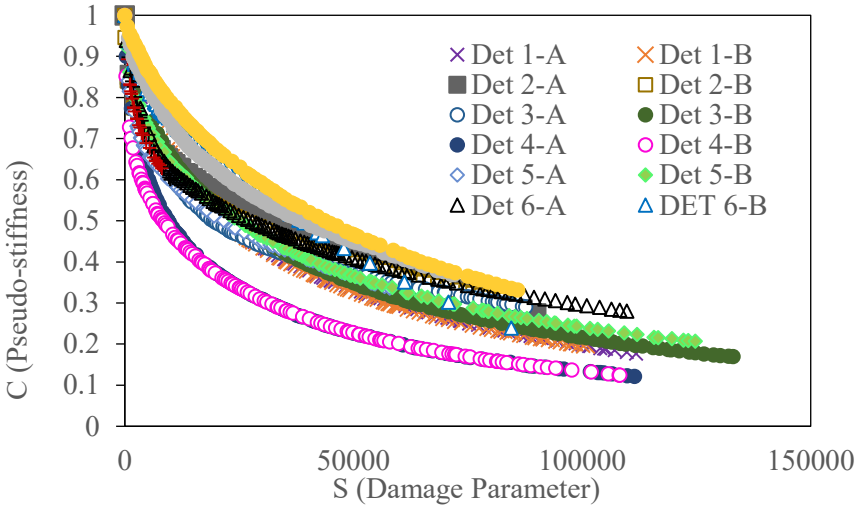

FIGURE 24 C vs S curves for all test runs.

Based on the statistical analysis, it can be concluded that except frequency, all other five factors have significant effects on the 3PBC test results. Air voids, clamp tightness and eccentricity were expected to have significant effects on 3PBC test results. The reasons for this are as follows:

- Samples with different air voids are compacted to different levels and therefore the damage accumulation mechanisms are expected to be different.
- Clamp tightness affects the main assumption used in the Timoshenko beam formulations for the 3PBC test. If the side clamps are not sufficiently tight, the assumption of the beam being perfectly fixed at two ends becomes invalid and the beam can become a simply supported beam, in which the Timoshenko beam formulations are different.
- Eccentricity in the central clamp will completely change the statics of the system and the stresses will be inaccurate.

These findings can be further validated with inter laboratory experiments with different mixture types at different conditions. Having these results, the research team would go for narrowing down the ranges of each factor so that tolerance levels can be recommended accurately.

TABLE 13 Ruggedness Test Results and Statistical Analysis for the 3PBC Test

Determination #	Air Void	Strain Level	Clamp Tightness	Temperature	Frequency	Placement of Central Clamp (Eccentricity)	Air Void	Rep 1 N_f	Rep 2 N_f	Avg. N_f	Difference (Rep1 – Rep2)
1	1	1	-1	1	-1	-1	1	6687	7260	6974	573
2	-1	1	1	-1	1	-1	-1	8077	9223	8650	1146
3	-1	1	1	1	-1	1	-1	4917	3774	4346	1143
4	1	-1	1	1	1	-1	1	489	426	458	63
5	-1	-1	-1	1	1	1	-1	5009	4974	4991	35
6	1	1	-1	-1	1	1	1	29111	29459	29285	348
7	1	-1	1	-1	-1	1	1	12299	14930	13615	2631
8	-1	-1	-1	-1	-1	-1	-1	18915	19028	18972	113
Avg+	12583	12314	6767	4192	10846	13059	12583			Std. error	1097
Avg-	9240	9509	15055	17630	10976	8763	9240			S_r	775
Abs. Main Effect	3343	2805	8288	13438	130	4296	3343			S_{effect}	388

TABLE 14 Statistical Significance of Effects for the 3PBC Ruggedness Test

Factors	Est. Effect	Student's t	p-value*	Half-Normal
Temperature	13438.2	12.26	5.52E-06	1.73
Clamp Tightness	8288.4	21.38	1.23E-07	1.15
Placement of Central Clamp (Eccentricity)	4295.9	11.08	1.08E-05	0.81
Air Void	3343.2	8.62	5.63E-05	0.55
Strain Level	2804.8	7.23	1.72E-04	0.32
Frequency	130.4	0.34	7.47E-01	0.11

**p-value is the two-sided tail probability of Student's t with seven degrees of freedom*
Factors with p-value (< 0.05) are statistically significant at the 5 % level

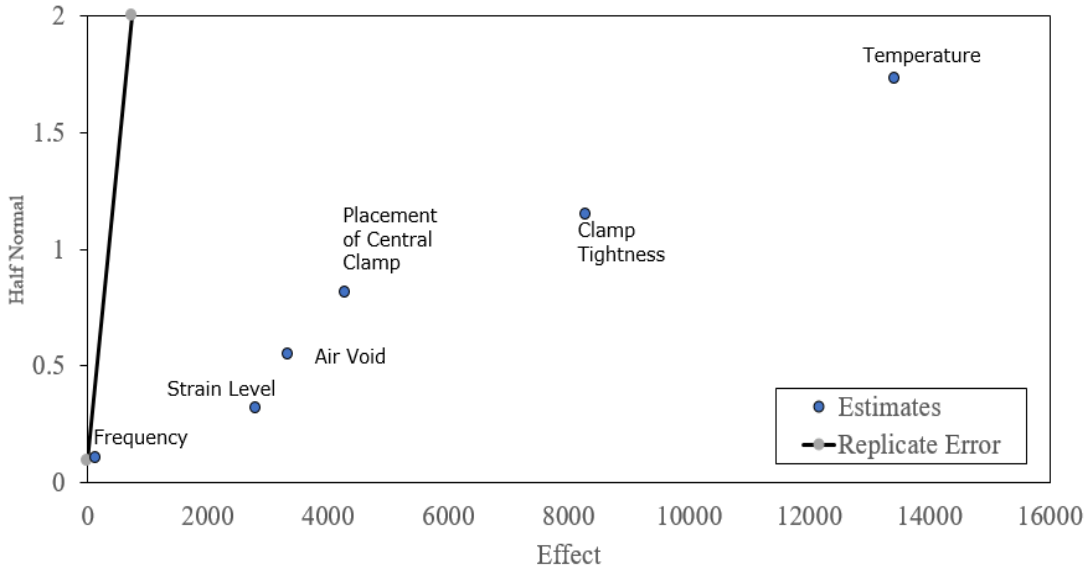

FIGURE 25 Half-normal plot for 3PBC ruggedness test results.

PLANS FOR IMPLEMENTATION

A draft ASTM standard for the 3PBC test procedure was prepared and sent to the ASTM D4.26 Fundamental Mechanistic Tests Subcommittee. The committee initiated a work item to evaluate the draft standard and several members of the committee had already provided their feedback on the draft. A collaboration area was set up on the ASTM website. Currently, the standard is being voted by the full ASTM D4.0 committee.

In the meantime, several universities showed their interest in the 3PBC test fixture and are willing to participate in an interlaboratory test plan. The test fixture will be transported with different asphalt mixtures with different aggregate sizes/types. The ruggedness factors and their corresponding levels will be further discussed and evaluated with partner laboratories. As mentioned before, the 3PBC test run is simple and time-efficient, thereby it does not require sophisticated and comprehensive training. However, required training for running a 3PBC test will be communicated via in-person lab demonstration or recorded videos.

A couple of companies potentially be interested in manufacturing the three-point bending cylinder test fixture (3PBC) and releasing the 3PBC test fixture commercially with the required software program which has already been developed. Therefore, this product will be easily available and help state agencies or any other consulting companies to evaluate asphalt mixture characterization while minimizing both costs and the time required.

CONCLUSIONS

The objective of this study was to introduce a more practical fatigue testing procedure compared to the traditional fatigue tests and provide data analysis approach based on the Timoshenko and Viscoelastic Continuum Damage (VECD) theories. This new procedure, referred to as the three-point bending cylinder (3PBC) test, addressed some of the challenges of the uniaxial fatigue tests. As part of this project, the 3PBC test device was improved, data analysis methodology was verified and validated using three-dimensional finite element (3D FE) analysis and laboratory tests. Two sets of ruggedness experiments were conducted to investigate the effect of various factor on the 3PBC test results. The findings of this study can be summarized as follows:

- Based on 3D FE analyses, it was shown that the error in elastic $|E^*|_{3PBC}$ ranges from 0.2 % to 16 %, whereas for viscoelastic $|E^*|_{3PBC}$ is less than 12 %. The results also indicate that typically, the error increases with the decrease in loading frequency. The 3PBC tests are recommended to be performed at 5 Hz and above, where the maximum error is less than 5 %.
- It was shown that the viscoelastic continuum damage theory can be used to model the fatigue life of an asphalt mixture at many temperature/frequency/strain level combinations, by simply running the 3PBC test at a single temperature/frequency/strain level combination. But it is recommended to run the 3PBC test at a few temperatures/strain levels to verify that C versus S curves collapse and there is no excessive sample-to-sample variability.
- The variation in the span length and air voids from 6% to 8% range did not have considerable effects on the fatigue life of the asphalt mixtures.
- However, the second part of the ruggedness study found that except frequency, other factors (temperature, clamp tightness, placement of sample, air voids (from 4% to 6% range), and strain level) had significant effects on 3PBC test results.

Overall, this test method possesses great potential to be considered as a routine fatigue cracking test. The method does not require cutting, gluing or on-specimen instrumentation. As a result, sample preparation and testing times of the 3PBC test method are shorter than typical fatigue tests (e.g., four-point bending and uniaxial fatigue) and the fixture is easy to operate and inexpensive.

REFERENCES

1. Hveem FN. Pavement deflections and fatigue failures. Highway Research Board Bulletin. 1955;(114).

2. Cowper GR. The Shear Coefficient in Timoshenko's Beam Theory. Journal of Applied Mechanics. 1966 Jun;33(2):335.

3. Timoshenko S, Gere JM. Mechanics of materials. New York: Van Nostrand Reinhold Co; 1972. 552 p.

4. Schapery RA. Correspondence principles and a generalized J integral for large deformation and fracture analysis of viscoelastic media. International Journal of Fracture. 1984;25:195–223.

5. Timoshenko S. Strength of materials Part 1. D. Van Nostrand Co., Inc,; 1940.

6. Du P, Lin IK, Lu H, Zhang X. Extension of the beam theory for polymer bio-transducers with low aspect ratios and viscoelastic characteristics. Journal of Micromechanics and Microengineering. 2010 Sep;20(9):95016.

7. Hutchinson JR. Shear Coefficients for Timoshenko Beam Theory. Journal of Applied Mechanics. 2001 Jan;68(1):87.

8. Schwartz CW, Li R, Ceylan H, Kim S, Gopalakrishnan K. Global sensitivity analysis of mechanistic–empirical performance predictions for flexible pavements. Transportation Research Record. 2013;2368:12–23.

9. Graziani A, Bocci M, Canestrari F. Complex Poisson's ratio of bituminous mixtures: Measurement and modeling. Materials and Structures/Materiaux et Constructions. 2014;47(7):1131–48.

10. Perraton D, Hervé ;, Benedetto D, Sauzéat ; Cédric, Quang ;, Nguyen T, et al. Three-Dimensional Linear Viscoelastic Properties of Two Bituminous Mixtures Made with the Same Binder. 2018;

11. Kim YR. Modeling of Asphalt Concrete. Kim YR, editor. ASCE Press; 2009.

12. Graziani A, Cardone F, Virgili A, Canestrari F. Linear viscoelastic characterisation of bituminous mixtures using random stress excitations. Road Materials and Pavement Design. 2019 Apr;20(sup1):S390--S408.

13. Kim YR, Seo Y, King M, Momen M. Dynamic Modulus Testing of Asphalt Concrete in Indirect Tension Mode. Transportation Research Record: Journal of the Transportation Research Board. 2004 Jan;1891(1):163–73.

14. Lee HS, Kim J. Determination of Viscoelastic Poisson's Ratio and Creep Compliance from the Indirect Tension Test. Journal of Materials in Civil Engineering. 2009 Aug;21(8):416–25.

15. Graziani A, Bocci E, Canestrari F. Bulk and shear characterization of bituminous mixtures in the linear viscoelastic domain. Mechanics of Time-Dependent Materials. 2014 Jun;18(3):527–54.

16. Rashadul Islam M, Faisal HM, Tarefder RA. Determining temperature and time dependent Poisson's ratio of asphalt concrete using indirect tension test. Fuel. 2015 Apr;146:119–24.

17. Camarena E. Evaluation of Poisson 's Ratio of Asphalt Concrete. 2016.

18. Maher A, Bennert T. Evaluation of Poisson ' s Ratio for Use in the Mechanistic Empirical Pavement Design Guide. No. FHWA-NJ-2008-004; 2008.

19. Tapsoba N, Sauzéat C, Di Benedetto H, Baaj H, Ech M. Three-dimensional analysis of fatigue tests on bituminous mixtures. Fatigue & Fracture of Engineering Materials & Structures. 2015 Jun;38(6):730–41.

20. Kassem E, Grasley ZC, Masad E. Viscoelastic Poisson's Ratio of Asphalt Mixtures. International Journal of Geomechanics. 2013 Apr;13(2):162–9.

21. ARA Inc. ERES Consultants Division. Guide for Mechanistic-Empirical Designof New and Rehabilitated Pavement Structures. Washington D.C; 2004.

22. Cao W, Mohammad L, Barghabany P. Use of indirect tension test and viscoelastic continuum damage theory for fatigue characterization of asphalt mixtures. Construction and Building Materials. 2018 Oct;187:38–49.

23. Graziani A, Di Benedetto H, Perraton D, Sauzéat C, Hofko B, Nguyen QT, et al. Three-dimensional characterisation of linear viscoelastic properties of bituminous mixtures. In: RILEM State-of-the-Art Reports. Springer Netherlands; 2018. p. 75–125.

24. Schapery RA. A theory of mechanical behavior of elastic media with growing damage and other changes in structure. Journal of the Mechanics and Physics of Solids. 1990 Jan;38(2):215–53.

25. Seitllari A, Kutay ME. Development of 3-point bending beam fatigue test system and implementation of viscoelastic continuum damage (VECD) theory. Asphalt Paving Technology: Association of Asphalt Paving Technologists-Proceedings of the Technical Sessions. 2019;88:783–810.

26. Bonaquist R. Refining the Simple Performance Tester for Use in Routine Practice. Refining the Simple Performance Tester for Use in Routine Practice (vol. 614). Transportation Research Board. National Cooperative Highway Research Program (Project NCHRP 9-29), Washington, DC; 2008.

27. ASTM E1169-20. Standard Practice for Conducting Ruggedness Tests. ASTM Standards. 2020;02(C):1–9.

28. Kutay ME, Lanotte M. Viscoelastic continuum damage (VECD) models for cracking problems in asphalt mixtures. InternatIonal Journal of Pavement engIneerIng. 2017;19(3):231–42.

29. Kutay ME, Hasnat M, Levenberg E. Layered nonlinear cross anisotropic model for pavements with geogrids. Advances in Materials and Pavement Performance Prediction II - Contributions to the 2nd International Conference on Advances in Materials and Pavement Performance Prediction, AM3P 2020. 2020;188–92.

30. Hasnat M. Calibration of the Performance Models of the AASHTOWare Pavement ME Design Software in Idaho. University of Idaho; 2019.

31. West R, Rodezno C, Leiva F, Taylor A. Regressing Air Voids for Balanced HMA Mix Design. WisDOT ID no. 0092-16-06, Wisconsin Highway Research Program, Madison, WI; 2018.

32. Harvey J, Tsai BW. Effects of Asphalt Content and Air Void Content on Mix Fatigue and Stiffness. Transportation Research Record: Journal of the Transportation Research Board. 1996 Jan;1543(05):38–45.

33. Norouzi A, Kim YR. Ruggedness study of dynamic modulus testing of asphalt concrete in indirect tension mode. Journal of Testing and Evaluation. 2017;45(2):601–12.

34. Bodin D, Terrier JP, Perroteau C, Hornych P, Marsac P. Effect of Temperature on Fatigue Performance of Asphalt Mixes. In 2010.

35. AASHTO R84. Standard Practice for Developing Dynamic Modulus Master Curves for Asphalt Mixtures Using the Asphalt Mixture Performance Tester (AMPT). 2017;13.

APPENDIX: RESEARCH RESULTS

Sidebar info

Program Steering Committee: NCHRP IDEA Program Committee
Title: DEVELOPMENT OF THREE POINT BENDING CYLINDER (3PBC) ASPHALT MIXTURE FATIGUE TEST SYSTEM
Project Number: 218
Start Date: October 4, 2019
Completion Date: May 31, 2022
Product Category:
Principal Investigator: M. Emin Kutay
Michigan State University
Email: kutay@egr.msu.edu
Phone: (517) 353 929

TITLE:
Development of an asphalt mixture fatigue test.

SUBHEAD:

This research study introduces a more practical fatigue testing alternative to the four-point bending and uniaxial fatigue tests.

WHAT WAS NEED?

Fatigue cracking is one of the dominant distress types that a pavement structure experiences throughout its service life. The current fatigue cracking tests are lengthy, cumbersome and expensive. Extensive material requirement for sample preparation, difficulty in meeting air void target, a large number of samples needed for testing, common premature 'end-failures' (leading to excessive sample preparation time and consumption of material), and high equipment cost are some of the challenges encountered when running these tests. To overcome some of these shortcomings, in this study a new test method called the 'three-point bending cylinder (3PBC) test' was developed.

WHAT WAS OUR GOAL?

Develop a fast and economical fatigue test system to determine the fatigue resistance of asphalt mixtures.

WHAT DID WE DO?

This research project developed a robust fatigue test system. This study showed the applicability of Timoshenko-Ehrenfest beam theory formulations to the 3PBC geometry, and it was validated via 3D Viscoelastic Finite Element simulations run at different temperatures and frequencies. As part of the study, the research team developed a test data analysis software. The software is named 3PBC-VECD. It is based on the popular viscoelastic continuum damage (VECD) formulations which reduces the experimental burden in calculating the number of cycles to failure (N_f) at different strain levels and temperatures. Moreover, a new testing protocol was programmed in the AMPT user programmable software to conduct 3PBC tests in the AMPT machine. The research team also conducted ruggedness tests to identify the major test factors that may influence the 3PBC test. Ruggedness testing is a key component in improving accuracy and developing test specifications.

WHAT WAS THE OUTCOME?

The three-point bending cylinder (3PBC) test was successfully developed alongside with drafting an ASTM test standard. A test data analysis software with step by step procedures were formulated. Some key findings and recommendations of this study can be summarized as follows:

- Based on 3D FE analyses, the 3PBC tests are recommended to be performed at 5 Hz and above, where the maximum error in elastic $|E^*|_{3PBC}$ is less than 5 %.
- For the viscoelastic continuum damage theory incorporation, it is recommended to run the 3PBC test at a few temperatures/strain levels to verify that C versus S curves collapse and there is no excessive sample-to-sample variability.
- The variation in the span length and air voids from 6% to 8% range did not have considerable effects on the fatigue life of the asphalt mixtures.
- However, the second part of the ruggedness study found that except frequency, other factors (temperature, clamp tightness, placement of sample, air voids (from 4% to 6% range), and strain level) had statistically significant effects on 3PBC test results.

WHAT IS THE BENEFIT?

Any research lab or consultancy firm can be benefitted by using this fast and cost-effective testing system worldwide. The developed test method can work as a screening tool in performance based balanced mix design process.

The benefit of this test method is that sample preparation requires less time, and it is easy to operate and inexpensive. Few other key features of this test method are: (i) no cutting, no gluing jig, and no instrumentation, (ii) no end failure as a result less material waste, (iii) well poised with AMPT and MTS units, (iv) relatively inexpensive test fixture < $2000, (v) minimum training required to operate the test, (vi) good repeatability with Coefficient of variance (COV < 10%), and (vii) test result is sensitive to asphalt mixture characteristics.

LEARN MORE

To learn more contact:

kutay@egr.msu.edu

IMAGES

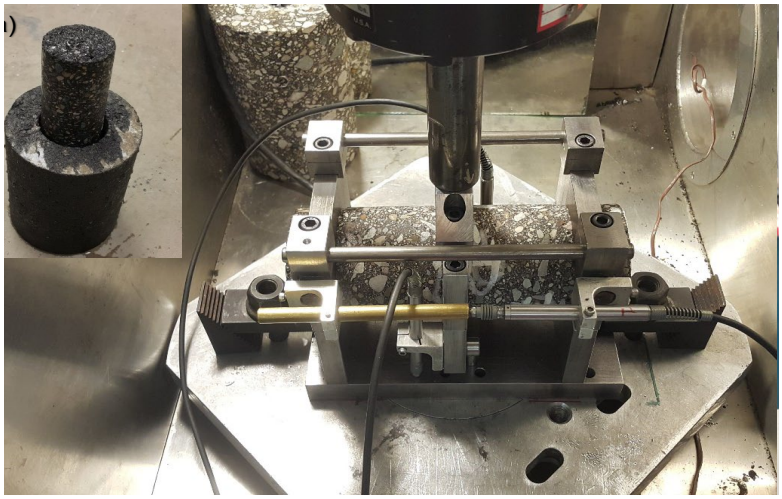

FIGURE A1 - *3PBC test setup with a loaded specimen in the Material Testing System (MTS)*

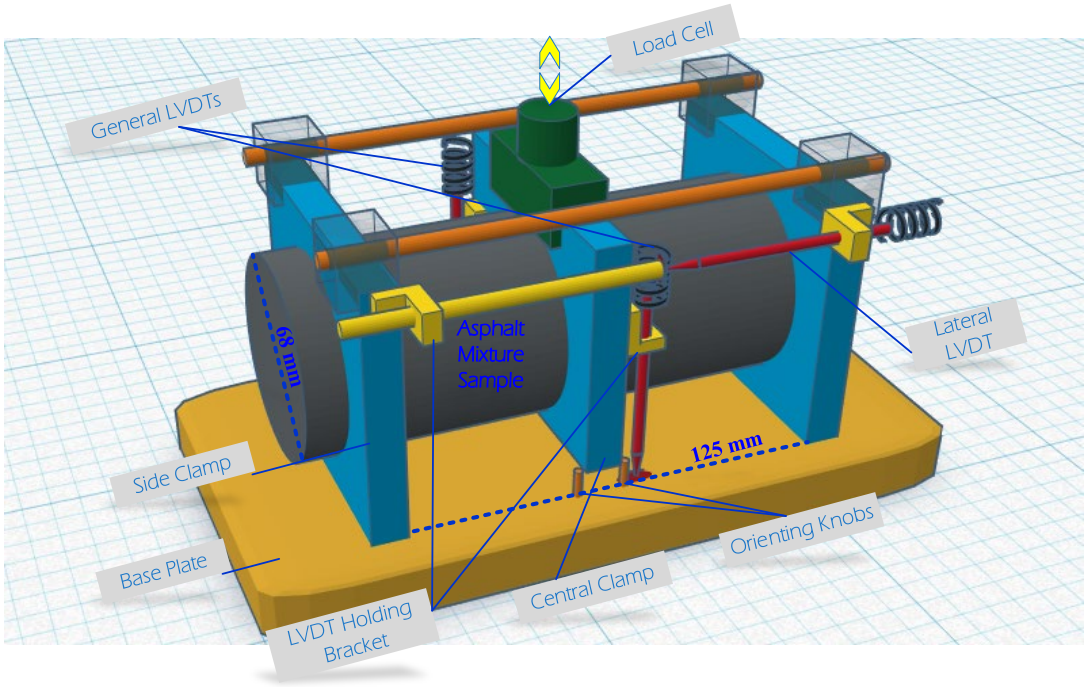

FIGURE A2 – *A schematic view of the 3PBC test setup*